Stringham, R. *When Bubble Cavitation Becomes Sonofusion*. in *237rd ACS National Meeting*. 2009. Salt Lake City.

When Bubble Cavitation Becomes Sonofusion

Roger S. Stringham
First Gate Energies, PO Box 1230, Kilauea, HI 96754

Experimentally, heat and ^{4}He are the fusion products of sonofusion (SF). SF controls a naturally occurring phenomenon with cavitation-induced bubbles and their high energy density transferred to transient jets that implant deuteron clusters into a matrix or lattice. The SF path to clusters can be extrapolated from high-density experiments of inertial confined fusion, ICF, Bose Einstein Condensates, BEC, muon fusion, MF, and astrophysical phenomena, to explain our ejecta sites, Qx, ^{4}He, and no measureable long-range radiation results. The fusion events emanate from deuteron clusters implanted into target foils. Clusters are squeezed and cooled via electromagnetic, EM, compression pressures and evaporative cooling of cluster surface deuterons producing the fusion environment. Evidence of these cluster fusion events is found in the millions of target foil ejecta sites in SF target foils.

Introduction (See Appendix list)

The first experiments in SF started early in 1989, although not initially known by that name, when the announcement of Fleischmann and Pons, FP, discovery was first announced. It was a week after the FP announcement that my first experiments began in cavitating D_2O with Pd targets. The initial experiments were at 20 KHz in large and cumbersome 20 Kg devices that over time – 19 years – are 1.6 MHz 20 gm devices with about the same excess heat output. Chronologically over the 19 years the size was reduced and piezo frequency increased for the evolving SF devices. And in the last ten years it was slowly realized that the high transient density of inertial confined fusion, ICF, and new astrophysical information, and the ultra low temperature bosons and fermions are linked and extended to SF. The SF cluster systems are 1000 times faster and billions of times smaller in volume and number of particles than the hot fusion ICF systems. The SF model is a series of sequential steps where the cavitation and jet are well established in mainstream science. The formation of transient clusters and their compression is more speculative in nature. And finally, the interpretation of ejecta site data is a logical interpretation of scanning electron microscopy, SEM, photos of ejecta sites found on target foils. These steps indicate a clear path to our SF experimental results [1] but may not be the only path. The emphasis of this model to explain the experimental fusion products of heat and ^{4}He is on the jet, the sonofusion cluster, and the ejecta sites

The environment of sonofusion is D_2O cavitated, Ar saturated, and reactor circulated. A target foil is carefully placed in the reactor. A cavitation produced cluster of BEC deuterons imbedded into the lattice serves as the containment of this nano scale transient deuteron cluster. The initially dense cluster is further compressed and cooled by evaporative surface deuterons of the cluster. These interact with free electrons forming deuterium atoms that surround the cluster. These accelerating free electrons produce an imploding spherical electromagnetic, EM, pulse that squeezes the cluster to fusion densities in less than a picosecond. And these electrons will pass through initially formed deuterium atoms to the fresh surface of the deuterons to keep the implosion pulse growing for about 0.1 picosecond. (The rate of formation of deuterium atoms is a femtosecond. [2]). The fusion event initiates a heat pulse destroying the cluster. The spherical heat pulse travels into and through the lattice to its surface. There it erupts with lattice ejecta and fusion products ^{4}He and heat, Qx. These products are measured by mass spectroscopy and calorimetry. Left behind in the target

foil are ejecta sites frozen in the target foil and easily analyzed by SEM. These ejecta sites can be related to the number of fusion events per site by their ejecta volume.

In the unique sonofusion, SF, process how are fusion products explained? One should consider high density systems like those of small white dwarf stars, WDS, where hydrogen fuel has been consumed. Its gravitational forces are not enough to ignite the remaining ^{4}He fuel putting the WDS on a 20 billion year cooling curve eventually sliding into a cold black dwarf star, BDS. Also MF density of the shrunken orbit of DDμ reduces the DD separation to the same separations as would be found in WDS and BDS via their gravitational forces. These are the densities that SF approaches [3]. DD muon fusion [4], which has about the same density or particle separation as a WDS and BDS, fuses deuterium at less than 100 K. However, local density between its two deuterium atoms in the muon molecule, DDμ, easily fuses the deuterium in the molecule. The two atom system, that is far below its Tc value with a big overlap of the de Broglie, dB, wavelength of DDμ two deuteron system does not possess the large heat sink of the SF cluster. The ability of the cluster to remove fusion energy as heat uses a different channel to produce ash products, ^{4}He and heat, as MF cannot distribute the heat of fusion to its surroundings as in SF. So it is expected that gammas will be in the products of MF and not of SF. The low mass of two MF deuterons does not compare to that of the mass of millions of SF deuterons in the coherent cluster and the heat transfer is very fast in the BEC cluster.

An interesting comparison between SF and MF is their densities and their BEC relationship. In a conversation with Steve Jones regarding his muon fusion experiments, he stated that the colder the deuterium the faster the fusion rate. The de Broglie wave function overlap of the two deuterons will increase at lower temperatures adding more coherence to the two deuterons in the DDμ+ fusion system decreasing the amount of contact time needed per fusion event in that chain reaction. This is the case if the cluster density is 10^{27} D+/cc. SF may react to the same circumstance, that is with regard to lowering of the cluster temperature via recombination, making a more favorable fusion environment [5].

New developments in inertial confined fusion, ICF, astrophysics and low temperature boson and fermion crossover physics help identify SF fusion paths. The SF path can be divided into series of six steps with some steps well documented and others new. The new are supported by new developing technologies in the above list. The transient high-density environment follows a natural picosecond process initiated by SF cavitation bubbles in water. When examining the density of matter that extends from the 10^{14} particles/cc found in ultra cold crossover systems to 10^{30} particles/cc found in BDS and DDμ, there is an obtainable upper end around 10^{27} particles/cc where the SF environment exist for a picosecond. The temperatures in this environment are relatively cool, below the critical temperature, Tc, for the density of the cluster being considered. The cluster temperature is mediated by the evaporation cooling of deuterons from the cluster surface, and the de Broglie matter wave overlap of deuterons in a BEC cluster. Deuteron cluster superfluids are produced in the unique transient SF target foil. The transient existence of this bubble produced cluster in the target foil has a DD separation of about 4.6 times greater than in DDμ of MF. The DD spacing of less than the de Broglie wavelength between deuterons occurs in both MF and SF clusters. The cluster consists up to perhaps a million deuterons. If the cluster temperature is less 32,000 K, the Tc for the deuteron BEC with a 10^{-9} cm separation, the cluster will begin to have some BEC characteristics. See figure 9. With these deuteron densities and temperatures the cluster is coherent and superconducting during its short lifetime. The coulombic repulsive pressure between the spin one deuteron bosons is overpowered by the EM pressures generated. Electrons are coulombically attracted to the large plus charge of the cluster.

The cluster deuterons surrounded by accelerated implanted electrons produces a spherical EM pulse focused at the center of the cluster that cools the superfluid via surface deuteron evaporation. The evaporation of cluster surface deuterons removes heat from the cluster during its compression. The densities of 300 gm/cc reached by the recent Backlighting experiments [6] were several times those found in the center of the sun but less by a factor of 100 of that calculated for SF. The picosecond flash implosion of high energy density cluster is squeezed by EM pressures of the million or less particles, contained in the cluster volume 10^{28}D+/cc or 33000 gm/cc, are contained in a target Pd lattice density of 12gm/cc with a gravimetric pressure of 50 atmospheres on the thin target foil.

The ejecta produces the millions of ejecta sites shown in scanning electron microscope, SEM, photos of exposed target foils. In the 1.6 MHz SF systems the period of this cycle is less than a microsecond. After implantation the fusion contact time of a picosecond is enough for a DD fusion event. This event will prevent any further fusion as it is destroyed by the DD fusion process. The initiated fusion heat pulse results in ejecta sites for low frequency cavitation systems. Ejecta sites are diminished in size as the frequency is increased. From the controlled bubble cavitation heat, ^{4}He, and ejecta sites are the experimental results on which SF is built.

With the above in mind, the system of cavitating D_2O in a piezo produced acoustic field creates cavitation bubbles as a precursor to high-density plasma jets, Bose Einstein Condensate, BEC, coherent clusters where fusion events occur. A good review of single bubble cavitation and densities produced during the collapsing bubble and other pertinent cavitation data about water bubbles in their final stages of collapse can be found in reference [7]. As the Mach 4 surface collapse of the cavitation bubble terminates the bubble, an ejection of some of the collapsed bubble plasma contents compresses and dissociates D_2O, forming high density jet plasmas. The dense plasma jet is injected into the cavitating D_2O via the bubble collapse and the jet accelerates as it implants into a target foil, where fusion occurs in squeezed and cooled clusters, followed by the fusion heat pulse that terminates the fusion locale while energy is removed from the foil by the generated heat pulse and ejecta. All of the above can be found in my earlier papers and in reference [8].

Sonofusion Process

The Cavitation Bubble

A quick view of cavitation and some of the basic information on the well-documented cavitation process that produces very high transient energy densities is reviewed. Cavitation is known to be a destructive force but in sonofusion this force is turned around to produce a DD fusion environment via transient cavitation bubbles, TCBs, in D_2O. A resonating piezo is the source of the driving acoustic power. The oscillator driven piezos produce a variable size bubble population where bubbles are naturally selected by their resonance properties using the parameters of pressure, temperature, and acoustic power. In recent years at higher frequencies of 1.6 MHz piezo reduces the damage characteristics found using lower frequencies. The initial bubble radius, Ri, grows isothermally, increasing its mass and radius to a maximum, Ro, followed by a violent adiabatic collapse to its final radius, Rf, producing sonoluminescence, SL, and a high-density jet. [8] These oscillator driven 1.6 MHz resonant bubbles are the naturally selected TCBs that violently collapse adiabatically in a single acoustic cycle. Millions of bubbles are created in one acoustic cycle. One cc of D_2O will increase in volume 1/10,000 with a million 4 μm Ro bubbles.

There is a tremendous increase in the bubble's energy density during its collapse, where the external pressure controls the initial energy density over the circulating D_2O. An adiabatic bubble collapse, a one hundred fold-decrease in the bubble radius without much change in the bubble's content mass leads to about a one million-fold increase in the bubble's energy density in one acoustic cycle. The jet has a sheath of electrons transferred from the bubble's interface. The jet is a high - density deuteron plasma and confined by EM pressures [9]. This is the first step in producing ^{4}He and heat in a sonofusion system.

Figure 1 shows an infant or initial TCB expanding in the D_2O and passing from the positive pressure half of the acoustic cycle into the negative half in an isothermal process picking up water vapor mass. The bubble continues on this path crossing again into the positive pressure half with a large gain in mass and volume size. At this point the partially evacuated bubble now at Ro stops its growth and in an inertial turnaround and a violent near adiabatic collapse process compresses to a radius of Rf. Here two things happen. The bubble emits a narrow pulse of SL photons, and the bubble produces a jet still encased by the bubble's interface. It is the SL that is measured and the jet with dissociated D_2O that implants into the lattice of the target foil.

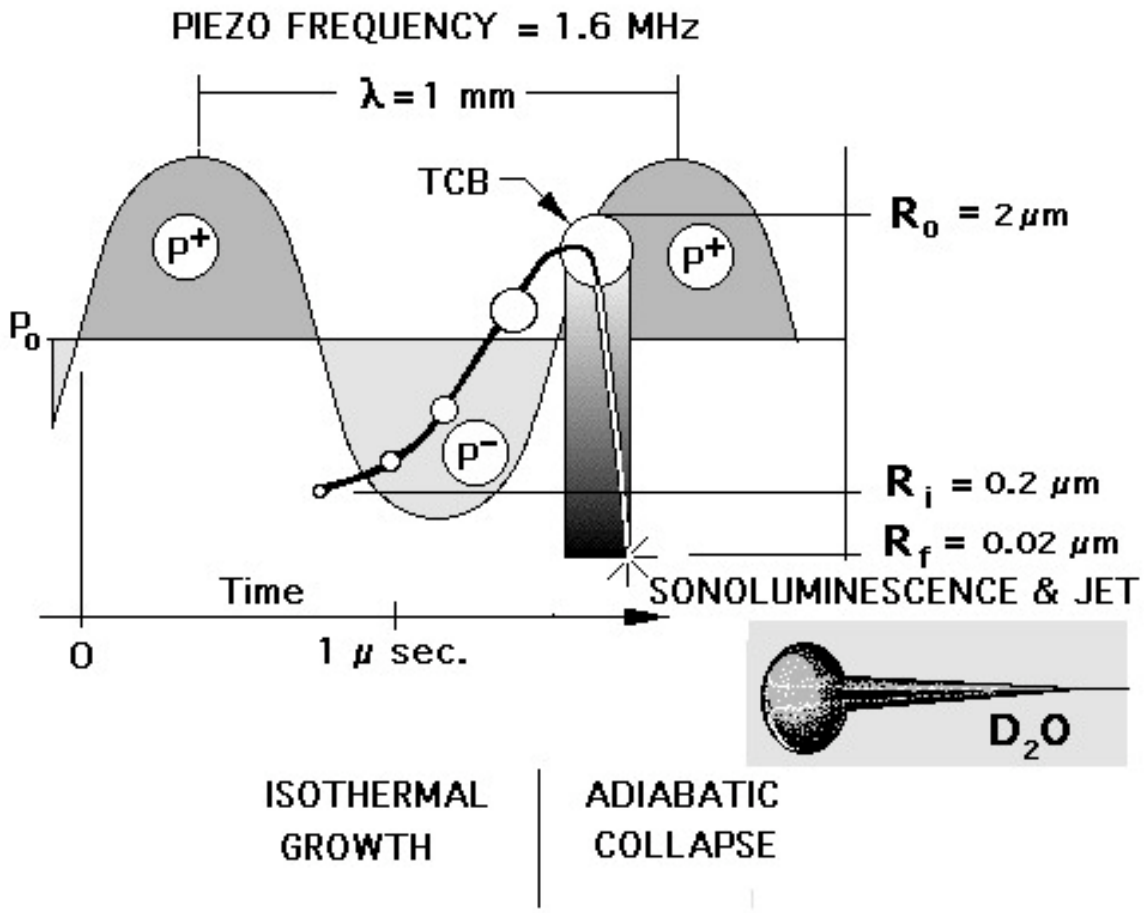

Figure 1. The cavitation process and its sonoluminescence. The TCB is produced in a closed D_2O circulation loop via a 1.6 MHz piezo where the TCBs rapidly grow gaining mass through rectified diffusion, and then collapse adiabatically. This one million-fold decrease in volume produces a one million fold increase in energy density. This is enough energy to dissociate the D_2O and to produce sonoluminescence and jet. See figure 2.

Jet formation and SL

The TCB bubble jet is formed by the violent collapse or implosion of the bubble in the cavitating D_2O acoustic field. The acceleration collapse process produces jets and SL. The SL monitoring system is a tool for looking at the plasma condition at that instant of photon emission measured with a PMT device. Managing the parameters of the running temperature, pressure, and acoustic input controls the plasma condition. Coincidentally transferring some of the plasma into an accelerating projection of the bubble interface forms a jet. This process lasts 100 picosecond or less.

There are many more jets formed than are implanted into the target foil and there are other geometries that may be superior but for the present the ability to observe SL with the disk configuration is necessary for control of SF. Only those jets within a few μm of the target will implant. The metamorphosis of the bubble into a jet have been photographed [10].

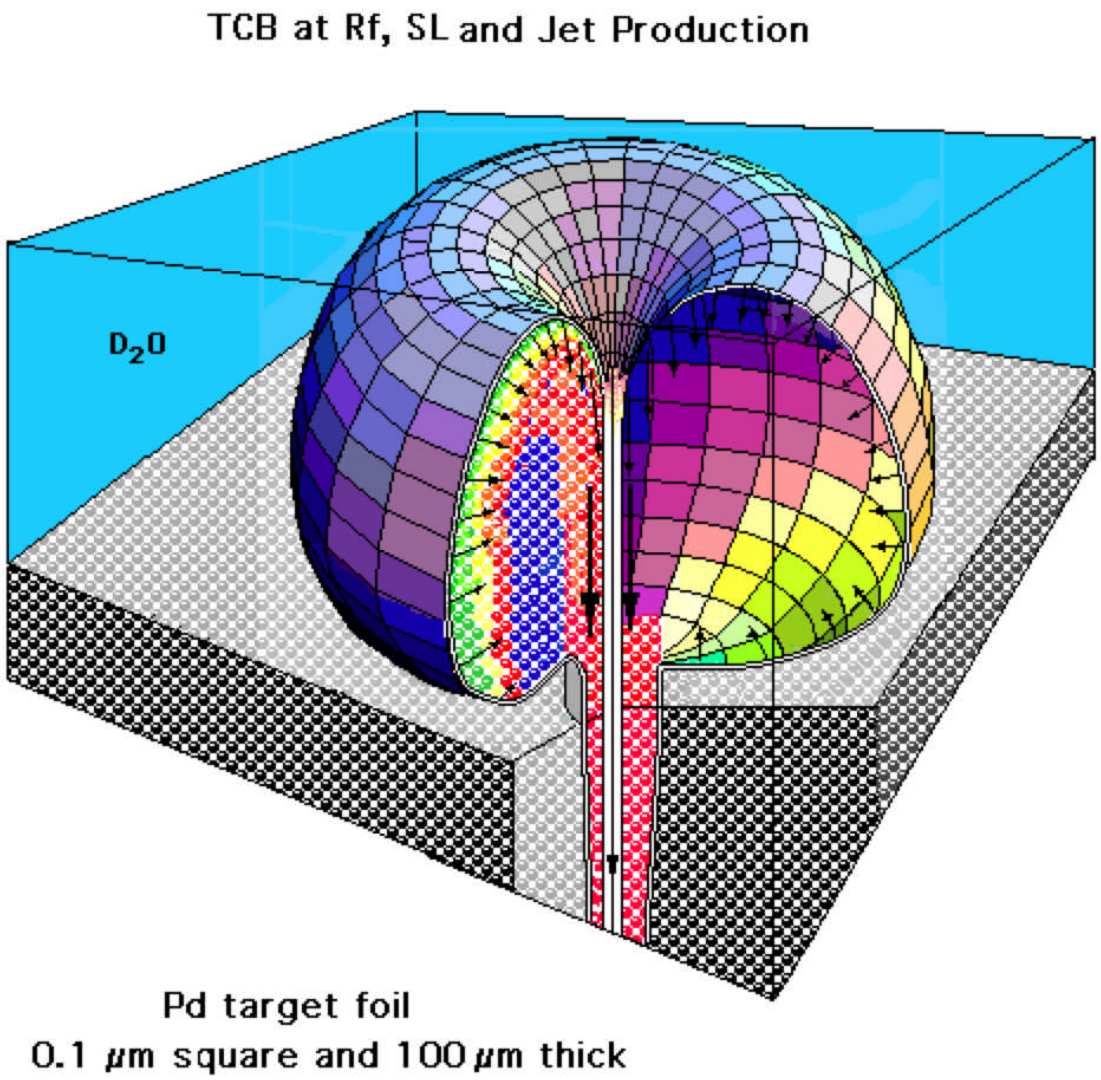

Figure 2. The final stage of the TCB collapse in D_2O and in a 1.6 MHz system. This occurs at the surface of the target foil or a few micrometers from the surface. In this figure the Rf cavitation bubble is cut away exposing the circulation of the bubble contents, the interior and exterior of the jet in the formation process, and the bubble interface. The spheres indicate the exchange of the hottest bubble contents being transferred to the jet. The compression heating of the contents bubble turns it into a partial high-density non-uniform plasma that accelerates the stretching the bubble interface and the most energetic deuterons and electrons into the high- density jets. The base diameter of the jet in this figure is about 100 μm for the lower frequencies (46 KHz). The base diameter for the 1.6 MHz would be smaller at about 10 nm and a volume 1000 times smaller. Note the direction of the Mach 4 imploding plasma via the arrows. The jet has several times that velocity. See the micro structure in figure 3.

The jet squeeze micro structure of the high density plasma jet.

Figure 3 shows the EM compression pressures that confine and squeeze the jet contents in the cavitating D_2O dielectric. In this short timeframe the D_2O will appear in this picosecond time frame as a glass dielectric, with the jet plasma passing through it. The jet is on its way to a target implantation.

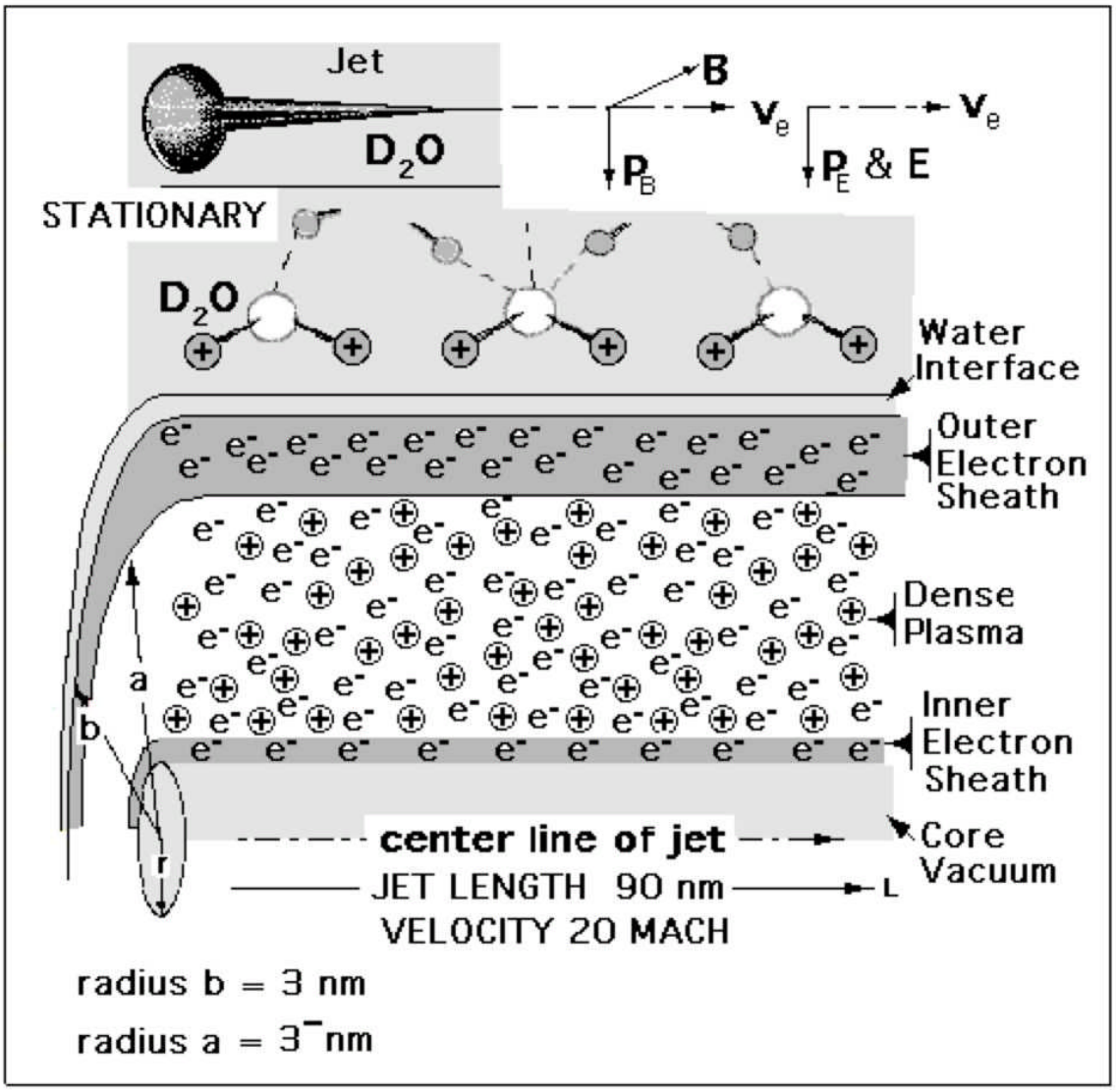

Figure 3. The details of the jet's complex content distribution and how it maintains its high density traversing the water dielectric. The escape pressure are countered by the electromagnetic, EM, pressures. The jet's characteristics have parallels to the experiments of imploding wires and the frozen D_2 fibers of the hot fusion community. The Mach 20 velocities of the sheath electrons, v_e, produce a magnetic field B with a force perpendicular to and towards the center-line of the jet. These sheath electrons also interact with the dielectric D_2O deuterons' partial charge producing an electric field, E, parallel to the magnetic field. The compressing pressures P_B and P_E further squeeze the jets contents over-powering the escape pressure of nK_BT/A.

During this passage the already dense plasma of the jet is further compressed. The interface between the surface tension oriented D_2O molecules, the deuterons oriented towards the sheath electrons, provides the geometry for the EM compression forces that pinch the jet contents. The velocity of sheath electrons and

the orientation of water's surface tension molecules provide for magnetic, B, and electric, E, containment fields. The concentric layer model of the jet plasma and its sheath electrons makes for a complex z-pinch of the jet's plasma contents and helps explain the jet's geometry. The jet is cylindrical, actually conical, construction consisting of a series of concentric layers starting with the outside water-proton interface, outer sheath electrons, the deuteron plasma, inner sheath electrons, and vacuum inner-core. During the several picosecond lifetime of the jet, it will implant the target foil before its natural z pinch destruction.

From the TCB metamorphosis the jet contents of deuterons and electrons are further compressed by electromagnetic, EM, pressures to higher densities in the order of 10^{25} D^+/cc via the 20 Mach sheath electrons. The jet implants into the target foil where the D^+ and e- are momentarily separated. The EM compression pressures confine and squeeze the jet contents in the cavitating D_2O dielectric. In this short timeframe the D_2O will appear as passing through a glass dielectric. The jet is on its way to a target implantation. During this passage the already dense plasma of the jet is further compressed.

Implantation and Cluster Formation

Figure 4 of the jet implant into the target foil and formation of the cluster. The impulse pressure of the colombically attracted cluster's free electrons produce an implosive EM pressure pulse that far exceeds for a picosecond the cluster's coulombic repulsion escape pressure. At the implant point of impact of the jet with the target foil those electrons loosely associated with the higher energy levels a deuterium atom were stripped of their electron via lattice stripping and are added to the populations of deuterons and free electrons. The charge separation process and the deuteron cluster containment immediately begins. There is a build up of deuterium the with the femtosecond recombination process as surface deuterons evaporate from the cluster surface controlled by the velocities and availability of free electrons.

The cluster is a coherent BEC collection of a million boson deuterium atoms, cooled by the evaporation of its exterior cluster deuterons. At 4000 K the D-D separation is 4 times smaller than its de Broglie wavelength and therefore obeys the BEC statistics. It is important to keep the temperature of the cluster low and with the help of evapoartive the squeeze on the cluster does not increase the temperature too much as the deuteron-deuteron distance is reduced by a factor of 10 approaching that of muon fusion.

The implanted deuterons and electrons are charge separated initially in the target foil lattice. They enter a dense plasma jet with the high impact of a meteor. This moment of charge separation is the start of the spherical implosion pulse that contains the cluster and does not permit its columbic repulsion of the high-density deuteron population in the cluster. The cluster consists of up to a million densely packed deuterons, a BEC plasma, surrounded by accelerating coulombic attracted electrons. Accelerated squeezing electrons may not penetrate the high deuteron density of the cluster and will react with an electron deuteron encounter that is removed from the neighborhood of the cluster. The surface is cooled by the continuous evaporation of deuterons from the surface of the cluster. The imploding spherical pulse of deuterium atoms and the EM pressures squeeze the cluster's deuterons. The evaporation removes cluster heat countering the heat of the pressure squeeze. This maintains a temperature below its critical temperature, Tc, of the dense cluster contents. This heat removal is important to the maintenance of the coherent BEC cluster keeping its temperature below its Tc. The coulombic escape pressure of the cluster is much less than the implosive EM pressure pulse during the cluster's picosecond lifetime .

The cluster coherence, superfluid, comes from the high-density low temperature of the cluster having a de Broglie deuteron wave several times the DD separation, 10^{-9} cm, in the very dense cluster. The BEC nature of the cluster alters the path or products of the cluster's fusion events products, which are heat and ^{4}He. If one compares MF and SF one finds the sonofusion DD separation can be driven close to that of MF. This path hopes to explain the results of Qx and ^{4}He the sonofusion experimental results. The difference is the ability of the SF BEC deuteron cluster to absorb the fusion heat pulse before any gamma can be produced. This is helped by the cluster's coherence. The cluster provides a large heat sink that immediately absorbs all the fusion heat because of its BEC wave function before any other available path. This is in contrast to MF that has only 2 deuterons of mass, not enough mass to alter its fusion products of neutrons, gammas and helium.

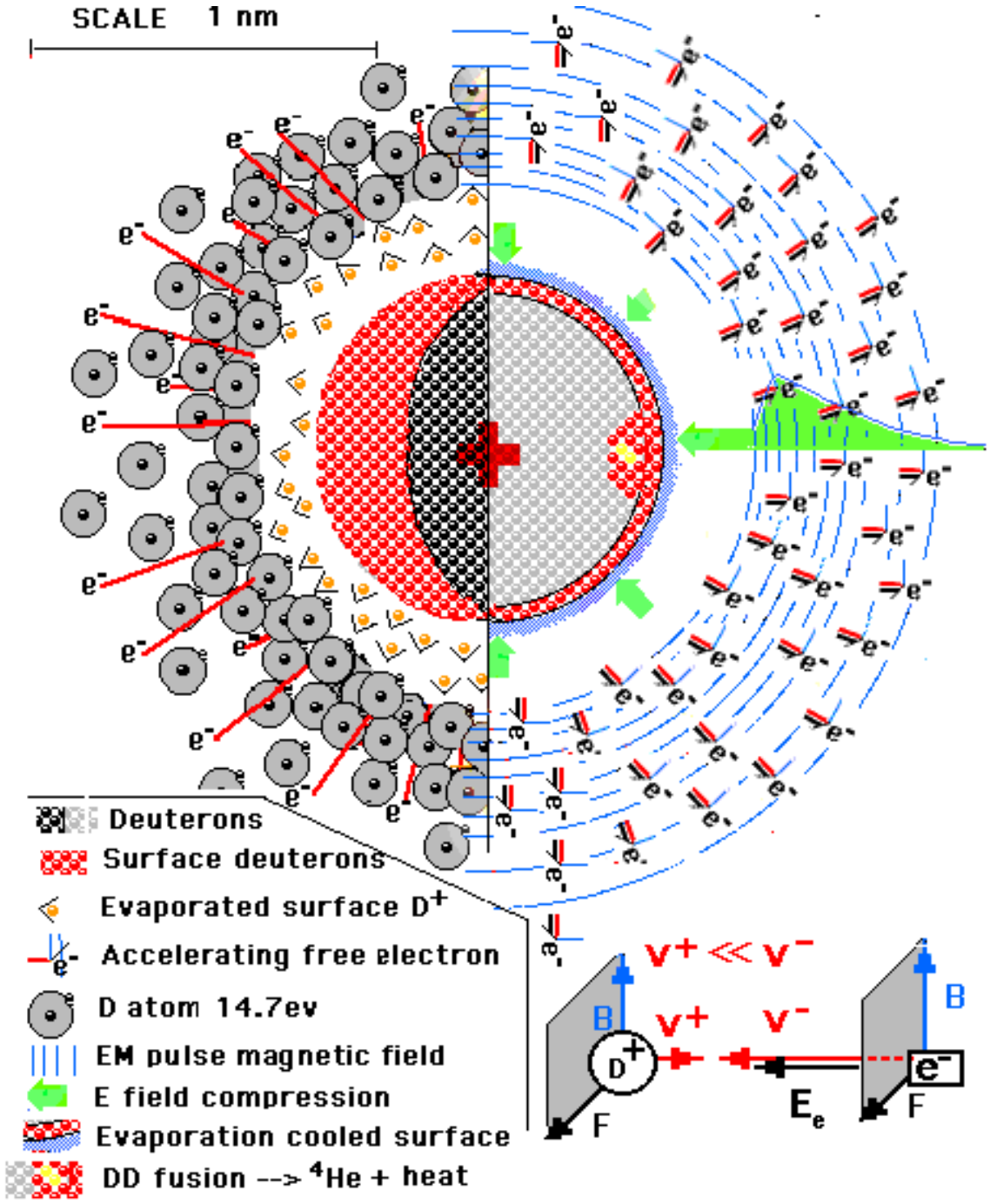

Figure 4. The implantation of jet electrons followed by deuterons produces clusters, gray and black dots – red dots are the surface deuterons. The green arrows show the EM implosion pulse compressing the cluster contents after implantation of the charge separated deuteron plasma. The cluster's black, red, and gray dots form an electron free sphere and is squeezed by EM magnetic containment and E compression pressure. The evaporative cooling deuterons, the tan dots with arrows, remove heat from the cluster and interact with the free accelerating electrons, gray deuterium atoms. Electrons compress the cluster with their picosecond E field pressure pulse that exceeds the coulombic deuteron repulsion pressure. The surrounding EM field, the blue lines, moves to the center of the cluster containing the imploding cluster.

After a picosecond the cluster has been squeezed to a BEC superfluid shown as the dots of the remaining interior and surface deuterons – ½ of the cluster dots become tan dots and are involved in evaporative cooling of BEC contents during the imploding pressure pulse. A good de Broglie overlap wave is produced giving the cluster BEC properties. A zone removed from the cluster sphere an evaporated deuteron may pickup an electron producing 14.7 eV away from the cluster. Fusion takes place probably near the cluster's surface, the red dots, the DD fusion takes place, yellow dots. A spherical fusion heat pulse immediately fills the cluster destroying the cluster and moving out and passing through the target lattice until it breaks out into the circulating D_2O releasing the heat and helium four. In the figure the lower left is the individual deuteron and electron and their EM contributions to the cluster squeeze.

The implosive EM spherical shockwave front initiates the SF events. During the passage of this shock front into the cluster a point will be reached where one or more DD fusion events occur. With the fusion event a much larger heat pulse, than the recombination to the D atom, is initiated and its energy is passed into the target lattice cluster that grows spherically, and upon reaching the surface of the target foil ejects the contents of the heat pulse into the circulating and cavitating water. The target foil is left with a problem of getting rid of the Qx heat and this problem is resolved by circulating the D_2O through a heat exchanger for the collection of Qx.

Cluster Summary

The confinement time in the cluster must be long enough for DD fusion events to occur and at densities of more than $10^{27 \text{ to } 30}$ deuterons/cc and a picosecond of contact time DD should produce fusion. This spherical shockwave impulse originates in a femto second timeframe. These deuterons in the cluster have a density approaching that of the MF $DD\mu^+$ at 10^{30} D^+/cc. The compression pressure heating is countered by the evaporative loss by deuterons leaving the cluster's surface deuteron layers [11]. The highly mobile free electrons produce EM compression implosion. The largest contributor to the compression is the E field implosion pressure that is developed by the same mobile electrons accelerating to the cluster surface. The spherical pressure wave pulse, a picosecond, compressing the coherent Bose Einstein Condensate cluster until a DD alpha fusion event(s) occurs destroying the cluster and initiating a spherical fusion heat pulse into the target lattice. The imploding shockwave sets up a transient environment that produces a DD fusion event and the resulting heat pulse and ^{4}He and Qx. For example if the first 10 surface layers evaporate producing a cooling and high implosion rate of squeezing in a Maxwell-Boltzmann type cluster shock wave in the high density BEC, there will be enough contact time for DD fusion to occur. The density of the transient cluster at the time fusion is greater than is more than1000 Kgm/cc. The expected gamma fails to mature because the heat of fusion is distributed between the remaining deuterons in the cluster before the gamma mechanism can produce a gamma. The cluster falls apart as deuterons and deuterium. These will quickly recombine in their expanding liquid neighborhood, mostly to D_2O.

The influence of Input Frequency to Clusters and Ejecta

The frequency changes influence of the acoustic input into the D_2O, bubble formation, and implantation. See figure 5 a. There were three frequencies used in the experiments of SF systems, 20 KHz, 46 KHz, and 1.6 MHz (A, B, and C). These had different ejecta size population distributions. See figure 5c. These target foil ejecta site distributions are related to their energy by the size or volume of each observed ejecta site. The SEM analyzes of foils is a simple way to observe the ejecta sites and make survey measurements of their size and number. The SEM photos show the ejecta site size distribution that range in diameter from 50 nm to 10,000 nm. The 50 nm diameter ejecta site equates to 20 MeV +/- 10 MeV as the ejecta site depth varies with the cluster deuteron implantation depth. The volume was calculated as the depth 2r times the ejecta area from a survey of a small surface area of typically exposed target foils at different frequencies. It appears that frequency (A) shows the most destructive collection of ejecta sites with the highest acoustic energy input and produced the largest number of fusion events per cluster from much fewer but larger clusters. The data for 20 KHz, (A), systems was extrapolated from (B) and (C) population distributions. The resolution of the SEM at A frequency was not good enough to view any site much smaller than a µm in

diameter. The damage at (A) was too severe to do a survey and the SEM resolution was only good to .2 µm. Only one example of an ejecta site was selected. See figures 5 c (A) and 6 a, b. Frequency 46 KHz, (B), survey showed a decided decline in the severity of ejecta damage of exposed foils and leads to the conclusion of fewer fusion events per cluster than (A). Frequency of l.6 MHz, (C), shows almost no visible damage except for a slight color change to the surface of the target foil. SEM photo of (C) and 6 e, f shows many small ejecta sites, about 50 nm in diameter, and a few larger sites and the highest concentration of the single event ejecta sites.

The energy density of clusters does not change with frequency but the number of clusters increases as their size decreases with increasing the acoustic frequency. But the number of fusion events per cluster at (C) is much smaller than at (A) or (B) frequencies. This explains the similarity of Qx at (A), (B), and (C) frequencies. The difference between population distributions of ejecta sites at the three frequencies is the number of fusion events per cluster found in the population surveys at the maximum number of ejecta sites for their population distribution at (A), (B), and (C). At the high frequency, (C), the fusion events are almost all single fusion events in the more numerous but much smaller clusters. Lower frequencies show, for example, at (B) the most frequent number of fusion events per cluster is around 10. And at (A) the most frequent number of fusion events per cluster is around 100. See figure 5 a. The number of single fusion events is present but not resolvable at the (A) frequency whereas (C) and (B) frequencies the resolution was good enough to see 50 nm diameter ejecta sites and produce the energy equivalent to one DD fusion event. Normally (C) produced one fusion event per cluster ejecta site.

The 50nm diameter ejecta site shows a population (C) of almost all single fusion event clusters. If the location of the cluster is too deep in the lattice there may not be enough energy in the heat pulse to reach the surface of the target foil in the Pd lattice. The heat will be distributed in the foil where it is removed by the circulating D_2O. However, a small amount of helium four may be captured in the lattice and will not be collected as a gas for analysis. This helium is still in the foil and can be analyzed at a later date. The conditions, 1.6 MHz, of (C) make the Pd target much more suitable for commercial use. What (C) loses in number of fusion events per cluster it gains from the increased number of TCBs and cluster production.

Note in figure 5 b the ejecta plume of target foil vapors leave behind 1 µ Pd spheres of condensed Pd at the ejecta site. The spheres are found imbedded on ejecta site walls and as free particles in and away from the site. The target foils in the (C) system, 1.6 MHz, are free of the 1 µm particles as the particles are larger in diameter than the (C) ejecta site diameters. Also the residual heat pulse is distributed into the target foil lattice and remelts the adjacent lattice and any earlier ejecta sites that may be in its neighborhood.

The SL PMT observation monitors the cavitating D_2O TCB's and their Rf final energy density provides a window into the collapsed bubble. SL in (C) appears to be brighter than (B) or (A). This can be partially explained by the great increase in bubble numbers produced by (C) at the expense of size. The many more but smaller bubbles have the same energy density and the same probability to fuse deuterons but the clusters are much smaller and so are the ejecta sites. It would be interesting to run some experiments at a frequency of around 200 KHz to look for a more intermediate target foil ejecta sites and the foils diminished lattice damage. See figure 5 c. The population distributions shift dramatically as the cavitation frequency changes.

The recondensed debris of small 1µ spheres associated with the larger ejecta and ejecta sites at (A) and (B) Figure 5 b. These spheres are the same size as the diameter of a 10 fusion event cluster. Therefore, in the smaller ejecta fusion events one will not find 1 µ spheres. SEM should view the residual lattice debris found in D_2O after the experiment searching for smaller sized spheres. The (C) events are present but may not be visible in the target foil (1.6 MHz). It is possible that the single fusion event may be too deep in the lattice and its heat pulse not break the surface of the target foil. See figure 5b. If that is the case one will find more helium remaining in the target foils.

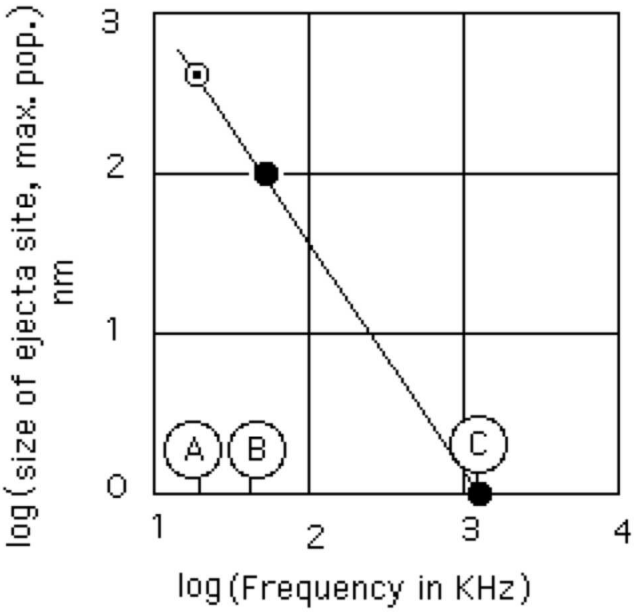

Figure 5 a shows the change in the energy of ejecta sites but not in the energy density.

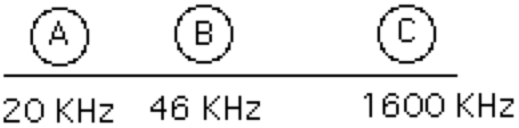

Older ejecta sites are destroyed as new vents are produced. See 5 b and the residual lattice heat.

Figure 5 c - the distribution of energy from clusters in the form of ejecta expelled from the lattice.

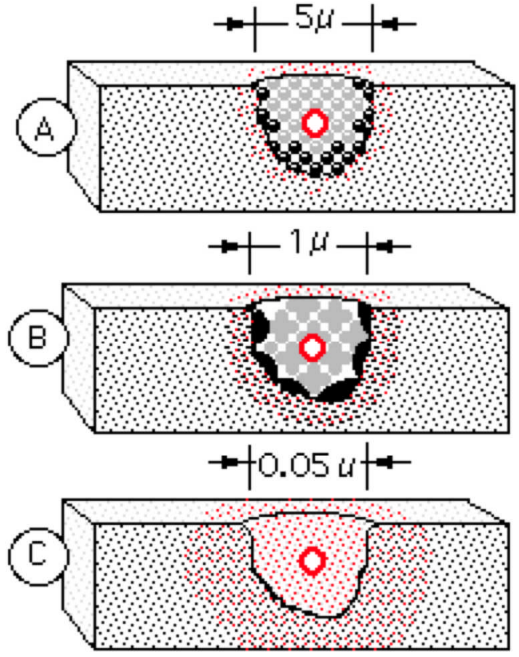

Figure 5 b the ejecta site after the heat-pulse has left the foil

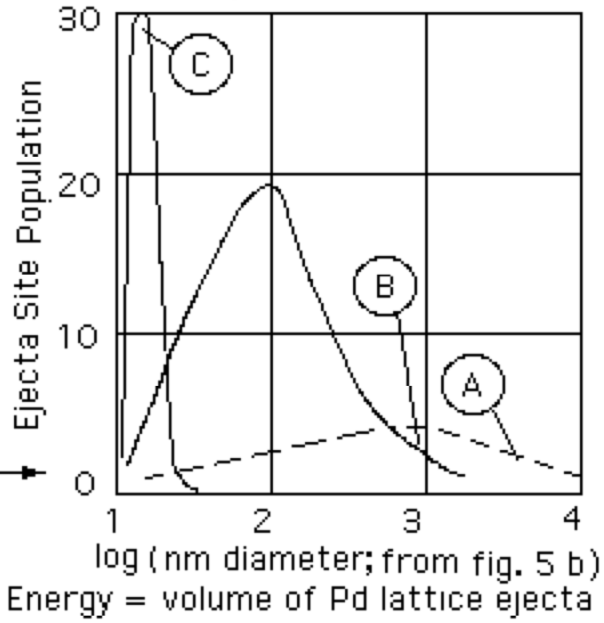

Figure 5. The collective information taken from SF experiments. There is a correlation that exists between the volume of ejecta, and the energy of the ejecta. Also, there is a correlation that exists with the TCB bubble size and the frequency of the acoustic input. Frequency's (A), 20 KHz; (B), 46 KHz; and (C) 1600 KHz produced decreasing population ejecta size distributions. Figure 5 a shows the log log plot of the acoustic input frequency vs. the diameter size of frequencies highest population size. This line is a straight line with point (A) calculated from 5 b (A). Figure 5 b is the representation of the typical ejecta site for a

given frequency. Note the 1 µm spheres were loose or partially melted into their ejecta site walls. However the foils that have ejecta site diameters of less than 1µm do not have this option. Note that not all the heat was in the ejecta plume, some was left behind in the lattice. The figure 5 c shows the population distribution curves from foil surface surveys at different frequency get narrower as the frequency is increased. Here you have the maximum for each distribution at 500, 100 and 1 as the frequency is increased. Also note the marked location of the three ejecta diameters of 5 b on the ejecta site distribution of the different frequency plots.

Figure 5 shows the consequence of squeezing the cluster by the recombination impulse and EM shockwave that together create a DD fusion environment. N is the number of deuterons converted to deuterium atoms during the recombination process generating the picosecond implosion shockwave. N may be as high as 10% of the cluster deuterons. At around 10^{-12} seconds the increasing pressure in the cluster provides the high-density low temperature environment for DD fusion. The implosion shockwave produces the alpha and the fusion destruction of the cluster. This is the start of the fusion heat pulse. The result of this heat pulse traversing the lattice of the target foil is millions of ejecta sites found in the SEM photos of target foils.

SF is an extremely high-density transient system and to date indicates higher densities than ICF hot fusion experiments, and except for muon fusion is an abbreviated version of an ICF system. The cluster, having a much smaller volume and higher density, requires a shorter fusion contact time than other ICF systems. It is advantageous for SF to draw from astrophysics, ICF, BEC and Bardeen, Cooper, Schrieffer, BCS, to help explain the SF path to fusion. When the density reaches 10^{27} D+/cc in the cluster the particle separation distance (10^{-9} cm) falls below that of its De Broglie wavelength forming a system of coherent BEC deuterons in the SF cluster. The cluster is squeezed by the electromagnetic, EM, pulse to achieve DD fusion. The comparative table of sonofusion and some of the better-known high density systems are found in Table I.

SEM Photos of Ejecta Sites

Figure 6 a and b are two FE SEM photos at 20 KHz (A) cavitation inputs exposing 100 µm thick Pd target foils exposed to cavitating D_2O at the Photosonication Lab in Woodside, CA. in 1993. The damage to this foil was extreme showing large events of the type in photo 6f where 10 µm ejecta site with loose 1 µm spheres were piled up inside its rim. See 5 c (A). Figure 6 a shows the general Pd surface terrain that needs to be resolved to make the ejecta survey count for the 1600 KHz exposed Pd target foil surface. This was not possible because of the foil destruction and the SEM resolution but a calculation was made to show the straight line plot of figure 5 a.

Figure 6 c and d are two FE SEM photos at 46 KHz (B) with cavitation inputs exposing 100 µm thick Pd target foil from a run at Stanford Research International, SRI. There have been many such foils and all show this type of ejecta damage. Only a few exposed target foils have been analyzed via SEM photos. About 50% of the target foil surface in the SF reactor comes in contact with the intense cavitation field that produces TCBs. The one square µm portion of SEM photo 6 d was surveyed and is typical of the surface of the 50 cm^2 exposed Pd target foil, which includes both sides (5x5 cm^2 foil). The surface here is typical of the Pd target foil surfaces that have been photographed for frequency (B). This survey includes 21 ejecta sites with a wide distribution of ejecta site volumes. See figure 5 c (B). Figure 6 c shows the general Pd surface terrain that needs to be resolved to make the ejecta survey count for the 46 KHz exposed Pd target foil surface in photo 6 d.

Figure 6 e and f are two FE SEM photos at 1600 KHz (C) with cavitation inputs exposing 100 µm thick Pd target foil from the First Gate lab in Kilaeua, HI. The 1.6 MHz reactor was only 20 gm compared to 5 Kgm for the 46 KHz device. The one square µm of the SEM photo 6 f was surveyed and a total of 30 sites were found with a very narrow population distribution that consisted of 29 50 nm diameter sites, single fusion events, and 1 multiple ejection site of 2 or 3 fusion events. This surface is much different showing no visual damage, only the very small events that appear not to loose target foil mass. See 5 c (C). Figure 6 e shows

the general Pd surface terrain that needs to be resolved to make the ejecta survey count for the 1600 KHz exposed Pd target foil surface.

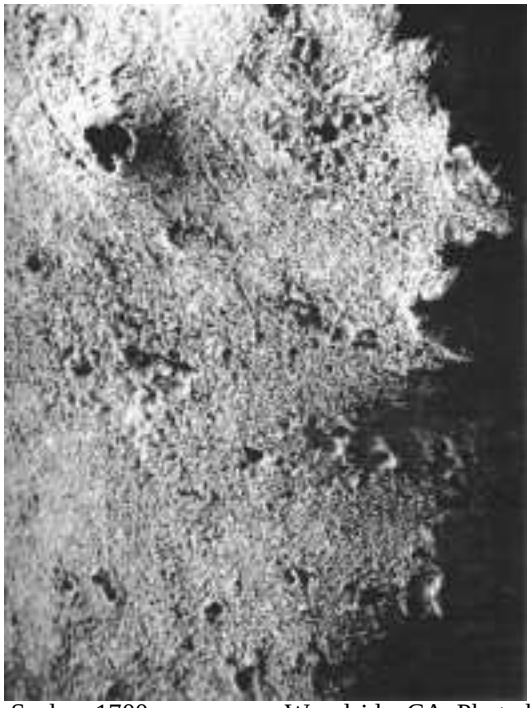

Scale _ 1700 µm; across. Woodside, CA. Photo by John Dash Scale 20 µm across.

Figure 6 a. SEM photo of a Pd target foil ejecta site at a frequency of 20 KHz shows the ejecta damage to the foil surface. (maybe some high density gravitational effects)

Figure 6 b. SEM photo of a n ejecta site 6a Pd target foil exposed to 20KHz cavitation shows one of the large multi fusion events showing the 1µm diameter sphere debris in the vent.

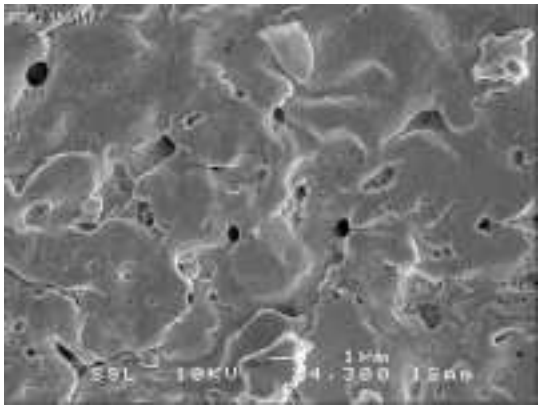

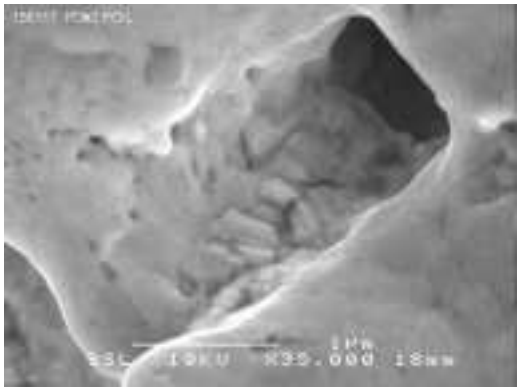

Scale __ 1 µm; Foil from SRI Menlo P., CA. Photos by Jane Wheeler Scale _____ 1µm Evans Lab., Sunnyvale, CA.

Figure 6 c. SEM photo of a Pd target foil ejecta sites at a frequency of 46 KHz shows the ejecta damage to the foil surface. Much milder damage than 20 KHz.

Figure 6 d. The SEM photo of several square µm of 6 c Pd target foil exposed to 46 KHz cavitation shows the diversity of the ejecta population.

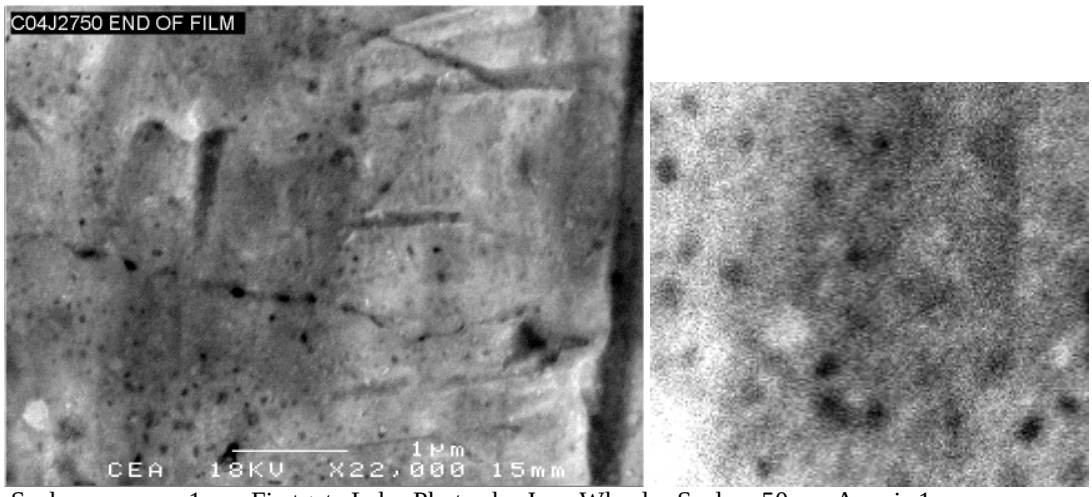

Scale _____ 1 µm Firstgate Lab.; Photos by Jane Wheeler Scale _ 50 nm Area is 1 µm square

Figure 6 e. SEM photo of a Pd target foil with ejecta sites at a frequency of 1.6 MHz shows the ejecta damage to the foil surface. The damage is minimal to the exposed foil

Figure 6 f. SEM photo of a square µm of 6 e Pd target foil exposed to 1.6 MHz cavitation shows the uniformity of the ejecta population in the 50 nm diameter range.

The SEM photos of SF target foils exposed to cavitating D_2O at different acoustic driving frequencies are shown in figure 6. These are the same frequencies described for figures 5 a, b, and c and represent typical SEM analysis photos and survey counts of ejecta sites of their distribution in a 1 µm square of target foil area and surveyed from SEM photos shown figures 6 a, b, c, d, e, and f. The SEM photos of figure 6 correlate with the figure 5 a, b, and c the three frequencies of (A), (B), and (C) and the photos. Correlation of photos 6 a, b, with (A) and photos 6 c, d with (B) and photos 6 d, f with (C). The figures 6 a,b were made by John Dash on his SEM device at Portland State University. The rest were taken by Jane Wheeler of Charles Evans lab. in Sunnyvale, CA, using a JOEL 6400 FE SEM with better resolution. A number of SEM photos were by Lorensa Moro at SRI but are not shown as most relate to other targets foils of different elements. There is a lot more SEM work to be done with 60 exposed target foils stored away. Only a few Pd foils are shown here but the sample is a good cross section for the demonstration of the acoustic frequency input.

Calculating the energy to vaporize and accelerate a volume of target lattice from an ejecta site into the cavitating D_2O was done for each of the ejecta sites found in a 1 μm^2 of (B) and (C) (the same results were found for other target foils). The calculation involves the velocity of the heat pulse in the Pd target, the energy of Pd atomization, and calculating the number of vaporized Pd atoms in the volume of the ejecta site. As an example, for a one fusion event ejecta site about 50 nm in diameter, the spherical heat pulse expands from the implanted fusion point in the lattice 25 nm below the surface of the target in all directions. This involves the fusion heat pulse expanding through the lattice to the target surface and ejecting the heat pulse contents into the circulating D_2O with a velocity of about 4000 m/sec and a temperature of about 4000 K. The energy in the heat pulse is in the order of 10^{-11} Joules for the 50 nm diameter ejecta site and the heat of vaporization for Pd is 377 KJ/mole for the 5×10^7 Pd ejecta. The instant the cavitation process is stopped the surface is frozen and allows for a leisurely SEM analysis of the foil surface. One often sees, via SEM, in the interior of the larger vent sites, 2000 to 10,000 nm in diameter, 1 µm meter and smaller diameter spheres of recondensed target foil that loosely coalesce in and on the target foil vent site surface. The path from the jet plasma formation to the ejecta site is reasonable, but not the only path to DD fusion.

Summary of Ejecta Sites

The SEM photos of the exposed target foils reveals differences in the ejecta site population with respect to the acoustic input frequencies (A), (B), and (C). (A) foils suffered the greatest cavitation exposure damage and had an ejection population that was dominated by clusters with high fusion event numbers. The SEM photos did not have the resolution, about a 0.2μm, for the low count fusion events (less than ten). (A) had the highest number of fusion events per ejecta site with a maximum of fusion events at a hundred or more. These large ejecta sites dominated the surface of the target foil. See figures SEM photos 6a,b. (B) foils had a better SEM resolution than at (A), about 30 nm, and more photons. One could get a reasonable survey of the ejecta site population at (B) foil SEM photos. This survey shows that the maximum ejeta site population is around 10 per site. When a comparison is made between the (A) and (B) it is obvious that the target surfaces are different and can be explained by the number of fusion events per ejecta site (this amounts to fusion events per cluster). See SEM photos at (B) figures, 6c,d. (C) foils visually showed no damage, only a slight discoloration, and the SEM analysis showed only very small pits on the order of 50 nm diameter. There may be a few a little bit larger that may result from two fusion events in a cluster that formed its ejecta site in the target foil. The population distribution for (C) is basically of single fusion events per ejecta. See SEM photos, figures 6e,f. The survey of (C) ejecta sites is from 30 sites from a 1 μm square area, 6f, from figure 6e. There were 29 sites with 50nm diameter single fusion event and one 2 fusion event site.

Calorimetry

A brief description of calorimetry in the running mode for the determination of excess heat was accomplished using the D_2O flow-through calorimetric measurements of the 1.6 MHz piezo driven low mass, 20 gm, device. See figure 8. Measure the temperature of the D_2O flow in and out of the device, □T, and its flow rate in cc/sec. and multiply these two together to give calories/sec. Multiply by 4.184 Joules/calorie to give the total heat out, Qo in watts. Now, Qo contains the 1.6 MHz acoustic input to the device, Qa, and excess heat, Qx. So Qo is the sum of Qa + Qx. The efficiency of Qi was measured at 0.33 (2) so Qa = .33Qi. To show the dynamics of Qx production, one can plot in real time the Qx production, Qo - Qa vs. Qi, is the same as Qx vs. Qi. Some of Qi powers a transformer and the 1.6 MHz oscillator. The efficiency of Qi to produce Qa = .33 Qi. The above is the basic calorimetry.

The spreading heat pulse contained the ^4He, Qx, D, and dominated by vaporized target foil atoms, which are ejected as a plume from the lattice around a minimum energy of about 20 MeV for the smallest ejecta site, into the circulating D_2O. These product gases are easily separated and collected and are measured by mass spectrometry. The heat was measured during the cavitation run as Qx using flow-through calorimetry above. Qx is the heat pulse that originates from cluster fusion events and via the fusion heat pulse and the ejecta is transported into the circulating D_2O and measured. See figure of the experimental set up, figure 8.

Discussion

Help for Sonofusion

A discussion of the experiments is covered by my earlier paper "Sonofusion, Deuterons to Helium, Experiments" [1] and lead to the model described in more detail here. The SF model is supported by ICF, astrophysics, ultra cold BEC, and muon fusion – BSC for light water. One can differentiate fusion placing them into two types of fusion events viewed from a commercial standpoint of heat producing systems. These are sustained events and one-time events. Sustained fusion found in the environments of stars and hot fusion reactors of magnetically contained plasma are continuous sources of fusion power (To date the latter has shown promise, but has not been an overall success.). The one time fusion event is a start and finish of a fusion event such as SF, fusion bombs, inertial confined fusion, and systems that self-destruct as they produce fusion events. SF is a self-destructive system of transient cavitation bubbles and their target implanting jets, containing about 10^7 particles in a volume of about 10^{-25} cc, where the following implanted cluster produces a one time high density fusion event. Ten trillion of the controlled SF bubbles a second initiate systems producing in the order of 10^{14} micro fusion events per second according to Department of

Energy, DOE, measurements of ^{4}He in product gases at a level of 552 ppm or 1.2×10^{18} atoms of ^{4}He during a 19 hour period [12]. This ^{4}He production occurs without any measured long-range radiation. It should be pointed out that in muon fusion at densities 10^{30} D^+/cc, fuses at temperatures below 100 K, to produce DD fusion. Sonofusion is a density driven system with the temperature control from evaporating cluster surface deuterons ions. Maintaining a low temperature is important for the formation of the BEC that is a system below its Tc. Boson particles, the deuterons in the cluster, are in their ground state. A SF DD density separation approches that found in a WDS or black dwarf star environment where if deuterons were present they would readily fuse at low temperatures 100 K or less. SF under the correct conditions approaches the density of forms of smaller WDS [3] and MF. These two are about equivalent. Other experiments that support this SF model are the many SEM photos of ejecta sites, calorimetric measure of heat, and helium four production.

Hot fusion parallels

A remarkable aspect of SF development is that of so much of the technology originates in hot fusion research and applies to the containment of the D^+ plasma in the SF jet and deuteron clusters in the target lattice. There is a slight twist and that is the temperatures must be kept low and the densities high and that is accomplished by the cluster EM implosion and surface evaporation process. In the hot fusion community with in-depth studies of sausage and kink pinches in the plasma that appear several milliseconds after the plasma initiation in relatively large Tokomak-like plasma systems are the unlikely keys to SF. These z-pinch forces actually compression the transient SF jet systems. The attempts for the various hot fusion systems to control the plasma with magnetohydrodynamics and electromagnetic fields applications to extend the plasma's useful life have failed to date. Continuous circulating hot fusion plasma was to be the answer for the world's growing energy problem. These results have been a major disappointment for the hot fusion community. But the z-pinch developing technology parallels the SF technology where pressure generation confines the TCB jet's transient contents into its long and pointed geometry and transient compression confinement times of a picosecond. Extrapolation of hot fusion z-pinch and imploding wire technology, especially deuterium frozen fiber high density z-pinch, HDZP, experiments [13] and ICF backlighting experiments [6] to SF has been very helpful in explaining some of the characteristics of the SF process. The pressures that hold, compress, and accelerate the jet plasma for its implantation into the target foil are parallel to the HDZP compression pressures. The scaling down of HDZP process to the jet size voume, 10^{-17}, will place these systems into the SF range. SF has the added advantage with addition of electric field pressures that compress the jet's contents further via the interaction of the jet's sheath electrons passing through the D_2O dielectric producing an E field. This is an advantage over the HDZP experiments as they are in a vacuum environment. A comparison of the HDZP and other fusion systems to SF has been made. Table 1. High-density plasma jets are natural constructions along the lines of a plasma capacitor with sheath electrons at the exterior and interior of the jet the D plasma. This jet construction is a transient multi-layer system [14]. See figure 2. In astrophysics the multi-layers refer to compartmentalized plasma systems often associated with Alfven waves [15**];** however, the SF jet is surrounded by the dielectric, D_2O, with the jet volume limited to the nano size range (90 nm long and 3 nm in radius for the 1.6 MHz jet). The jet with a velocity [16] in the Mach 20 range (30 k/sec) produces EM fields that contribute to acceleration and z-pinch shaping of the SF jet and is viewed as an extrapolation from the HDZP experiments [6]. Recent work in backlighting experiments in 2008 show the transient production of EM fields of 10^9 V/m and 60 Tesla in their inertial fusion implosions [6]. These experiments produced compressed densities of 300 gm/cc, more than is found in the center of the sun. Assuming liquid deuterium has a density of 0.19 gm/cc at one atmosphere, the density of the starting cluster for SF is around 3+ K gm/cc or 10 times more than the backlighting experiments. These inertial confined backlighting laser crushed capsules, similar to the forces on the SF cluster, but are much larger in volume and larger in number of deuterium atoms encapsulated. These hot fusion ICF projects have demonstrated the tremendous electromagnetic confinement pressures on hydrogen isotope systems. The 10^6 deuterons, the contents of the SF clusters, are compressed by EM forces more effectively than in the high current discharge or backlighting experiments. SF has a great 1 plus 2 compression punch with the jet compression followed by the cluster compression.

The SF fusion device

The 1.6 MHz SF device is small at 20 grams driven by a piezo 2 cm in diameter with a 1 sq. cm target foil, a window, and ports for thermocouples, circulating D_2O, oscillator input, calibration heater, and Ar pressurization. The body is machined from polycarbonate and sealed by squeezing the O-ring seals. See figure 7. Early devices were more massive around 10 Kgm of steel and acoustic horns and an equally massive power supply that drove the 20 KHz acoustic input into the circulating D_2O. By increasing the piezo frequency of the device to 1.6 MHz both the device mass and the power supply are reduced equivalently. The fittings were Omnifit or other similar small high pressure fittings. In some cases the window a 40 mil polycarbonate sheet. The calibration heater was a small, 0.0031 mills, high resistance wire 3.3 ohms/cm from MWS wire industries. The watts measured via DC voltage and current input the same as the watts to the oscillator, Qi, that drives the piezo.

In this 1.6 MHz device a bubble, jet, implant, cluster, fusion, and ejecta are formed in one acoustic cycle at a rate of 1.6×10^6 per second using a 1.6 MHz piezo. (This number is frequency sensitive. See figures 5 and 6.) The small 20 gm device produces 40 watts of Qx with 50 watts of input. A total output of 90 watts can be recovered as heat measured calorimetrically [1].

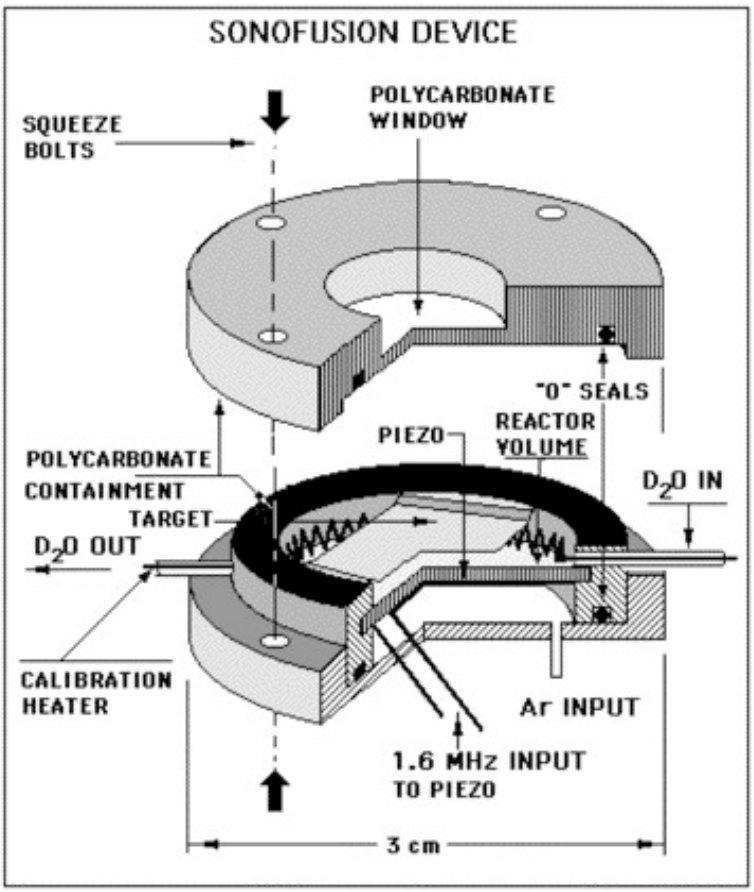

Figure 7. A schematic of a 1.6 MHz SF device with polycarbonate containment and window and its geometric configuration is shown. The physical orientation while running the device would usually be rotated 90^o, with the window perpendicular to the earth's surface with the input at the bottom. The general configuration is of concentric elements squeezed together with nylon bolts forming a watertight reaction chamber for the circulating cavitating D_2O. The piezo is clamped by the same squeeze that holds the target foil in place. The D_2O inputs and outputs are arranged so that there is a pulsing pressure in the cavitating D_2O that originates from the FMI circulating pump in the 1 cc reaction volume. Ar pressurization of the circulating water reactor and the space to balance the pressure on the backside of the piezo is useful in higher-pressure runs. The two electric leads from the 1.6 MHz oscillator power the piezo, which produces

the piezo acoustic input, Qa. The squeeze bolts provide a seal for the Ar that makes for a watertight device. The polycarbonate window piece with the "O" ring gasket seals the reaction volume. The window allows for the count of SL photons via a photomultiplier, PMT. With the squeeze in place the target foil is held tightly and acts as a shield for the window, blocking most of the cavitation's activity from damaging the SL window. The high resistance wire calibration heater is placed peripheral to activity of the 1.6 MHz acoustic fields generated in the circulating water.

The Circulation system

The SF device's target foil where the deuteron cluster is implanted into the lattice of the target foil is like a nano boson charged star. This transient star-like cluster is contained on the order of a picosecond, where its high-density coherent environment produces a SF event(s). The device where this SF occurs is a 20 gm system shown in circulation system in figure 8. The D_2O flow in and out of the SF device at measured temperatures, pressures, and acoustic inputs is crucial to watts out, Qo, and Qx measurements. Refer to the section on calorimetry for the details on the measurements of Qx for this device. The overall setup for these Qx measurements are shown in the circulation of D_2O through the various components and the data gathering system in figure 8.

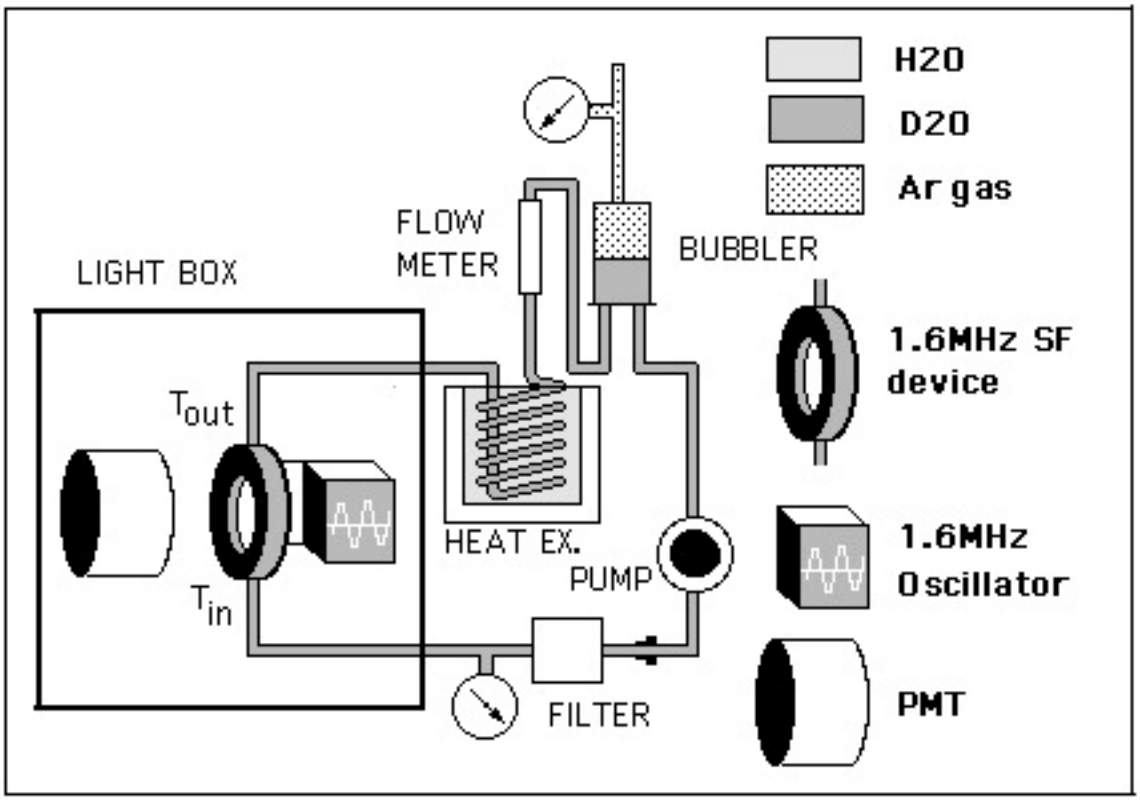

Figure 8. The experimental SF system was set-up to measure calorimetry via the temperature difference between the input and output. The two measurements Tout – Tin = □Tss, and the D_2O flow are the two parameters that complete the calorimetry measurement. D_2O flow x □Tss x 4.184 product is the measure of Qo watts, the output from the device. The system consists of the following components and their function. The 1.6 MHz piezo oscillator device, shown as a cube with sine-wave, drives the piezo producing the acoustic input, Qa. The D_2O, dark-gray, is circulated through the device at a constant rate by the mass flow FMI pump. The D_2O is saturated with Ar in the bubbler, the rectangle in the upper right. In the circulation line are the pump, filter, SF device, heat-exchanger, flow meter, and bubbler in that order. The

heat-exchanger's H_2O, light gray, removes heat from D_2O maintaining a steady state temperature in the SF device as the D_2O circulates. The PMT is shown as a solid cylinder, measures the level of SL photons that indicate the condition of the plasma in the final stage of the TCB collapse. These experiments required complete darkness and were done in a light proof box (no outside light interference) with circulating air maintaining a constant running temperature for Tin and Tout during experiments. The parameters that control SL are the temperature of the D_2O, the pressure of Ar over the D_2O, and the power of the acoustic input from the 1.6 MHz oscillator.

The comparison of SF to Hot Fusion

Support for SF comes from developments of the astrophysics of white dwarf stars and the workings of the Pauli Exclusion Principle, the BEC, and the nuclear ground states of deuterons. In Table 1 there is support from high-density z-pinch, HDZP, experiments [13] that can relate to the SF high-density jet, also the OMEGA backlighting experiments [6] in 2008 pointing out the very high transient EM fields produced in their ICF work. Muon fusion's low temperature, less than 100 K, and DD spacing of 10^{-10} cm compared to about 10^{-9-} cm for SF makes fusion possibilities realistic.
Table 1.

POINTS OF COMPARISON	HDZP D2 fiber	SONO	MUON	TOKAMAK	BACK LT. ICF; OMEGA
(1)Current 10^6 amps	2	10^{-6}	———	1	Laser
(2)Time in μ sec. (□)	0.1	10^{-6}	.001	10^{7}	0.001
(3)Length μm	$5*10^{4}$	0.1	10^{-4}	$6*10^{6}$	———
(4)Radius μm	40	0.003	10^{-4}	10^{6}	430
(5)Density D_o/m3	Solid D2 $5*10^{-28}$	D in D2O	D2 liq. $5*10^{-28}$	———	$5*10^{28}$
(6)Density cluster D/m3		10^{32}			
(7)Density D_f/m3	10^{30}	10^{32+}	10^{36}	10^{22}	10^{32}
(8)S_o/S_f	30	31	207	1	12
(9)Num. of particles	10^{18}	10^{6}	3	10^{23}	10^{13}
(10)D—D Separation S_o in m	$3*10^{-10}$	$3*10^{-10}$	10^{-10}	——— ——	10^{-10}
(11)D—D Separation S_f in m	10^{-11}	10^{-11-}	10^{-12}	10^{-5}	$2*10^{-11}$

Table 1 compares some fusion systems and through this process shows that sonofusion compares favorably. HDZP is the high-density z-pinch system and uses a 50 μm diameter frozen fiber of D_2 or TD. Using discharge capacitors a high density shaped current is discharged into this vacuum contained fiber creating an inertial confined wire system [13]. This z-pinch system parallels the SF jet just before it implants. SONO is sonofusion, a cavitation process, that is an ICF system but 10^{17} smaller in size than HDZP and the SF jet relies on its z-pinch effect. The jet is derived from the collapse of the TCB's high-density jet plasma that is implanted into a target foil producing a deuteron cluster fusion environment. MUON is muon fusion that substitutes a muon for an electron in the DDμ molecular ion□□□. This ion has the density equivalent or

separation of a white dwarf star and fusion occurs easily at low temperatures (40 K). TOKAMAK is the torroidal fusion reactor. Fusion lasted a fraction of a second before failing to the z-pinch effect. BACK LT was an ICF experiment using the OMEGA laser system for deuterium capsule compression. The discovery of nanosecond EM fields during the implosion process is a good fit with the cluster of the sonofusion process [6]. The subscript "o" and "f" (separation at time 0 =S_o) refer to initial and final conditions of implosions. There are 11 physical categories of comparison, but the most striking comparison, not shown, is the economics of sonofusion that is close to being market competitive

The de Broglie Wave

The fusion activity focuses around the boson cluster. The clusters must possess low temperature and high density for de Broglie matter waves overlap of the ground state clusters' deuterons. This gives the cluster coherence and the ability for the clustered deuterons to act as a single entity, a super fluid. Figure 9 shows for a given density or separation of 0.01 nm the Tc temperature value for a coherent deuteron cluster.

Figure 9 is a graph at constant deuteron cluster density with increasing temperature. The cluster is a coherent BEC collection of a million boson deuterium ions, cooled by the evaporation of its surface deuterons. At 4000 K the D-D separation is 4 times smaller than its de Broglie wavelength and therefore obeys the BEC statistics. It is important to keep the temperature of the cluster low, and with help of evaporation the squeeze, increasing EM pressure, on the cluster temperature is kept in check as the D-D distance is reduced by a factor of 10 approaching that of muon fusion.

In SF, immediately after implantation, transient charge separation of deuterons from the mobile electrons creates a very dense deuteron cluster in the target lattice. The cluster is in the target lattice, but in an isolated dense transient plasma phase. If the cluster is not a BEC yet it will soon as the EM implosion pulse progresses. Figure 9 shows the de Broglie wave overlap in a deuteron cluster, where the de Broglie wave length exceeds the DD cluster separation. If the cluster's Tc temperature drops below 32,000 K via its evaporated cooling and its DD separation is 0.01 nm in the boson cluster it starts changing its phase following Bose Einstein Statistics on its way to a BEC. In the figure the de Broglie wave-length varies as $h/T^{0.5}$ so at 8,000 K the dB wave length is 2x the cluster separation. The cluster density in the figure is placed at of 10^{27} D+/cc. For example for a cluster temperature at 2,000 K with a 4 x dB overlap it is a coherent BEC cluster providing an environment for the SF of $2D^+ \rightarrow$ Qx and ^{4}He. There will be no gammas because the boson-cluster acting as one atom, a superfluid, and its wave overlap will distribute the DD fusion energy to the cluster as heat, before the gamma mechanism can take place [17]. The 5.7×10^{21}cyc./sec gamma does not compete with the superfluid conductivity. This heat is the Qx of the sonofusion process that is measured by calorimetry. A plasma cluster environment should be commonplace in the cooler astrophysical star community [18].

In conjunction with the fusion heat pulse ejeta sites, there is a continuous bombardment of new cluster heat pulses in the lattice on top of older sites that will melt and erase these sites. See figure 5 b. There was enough residual heat to remove previous neighboring ejecta sites. Residual ^{4}He retained in the Pd target foil that did not escape via the ejecta plume and was measured at 10^4 times greater than the one would expect from the 5 ppm found in air during Pd foil's manufacture [19]. This ^{4}He near the ejecta sites but still retained in the lattice was located possibly in the site walls of the ejecta sites. The amount measured in one analysis was low, around 10^{16} maximum. ^{4}He atoms in Pd target foil are about 100 times less than found in the foil gas phase measurement. (note: There should be more MS analysis of the 1 μm debris of target foil ejecta spheres for helium four residual as well as exposed target foils.)

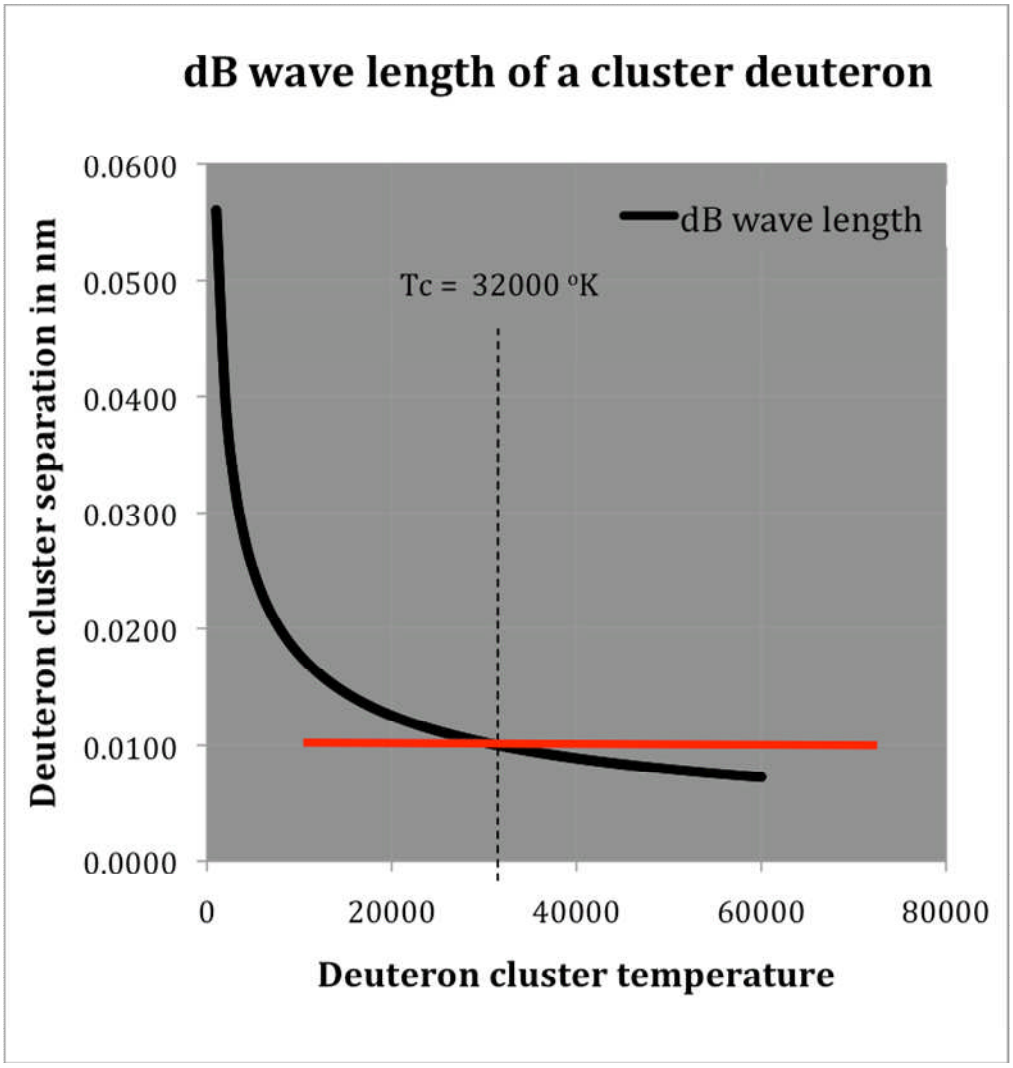

Figure 9. A graph of the probable deuteron cluster temperature before the fusion event vs the deuteron separation in nm. In this case a Tc value of 32,000 K for a cluster deuteron separation of 0.01 nm is represented by the red line. The black line is the de Broglie wave-length and overlaps the DD cluster separation up to the cluster's Tc where a phase change occurs. Any further increase in the cluster's temperature will follow the normal Boltzmann statistics. The system is a coherent BEC deuteron cluster as its temperature increases until it reaches the dotted line. The deuteron cluster is a normal plasma after the temperature passes beyond Tc. It is important that the cluster temperature is kept cool by the evaporation of deuterons from the cluster surface. The cluster provides density conditions for DD fusion events with the fusion products heat, Qx, and ^{4}He as the preferred fusion products. No gamma radiation was found with the experimental production of ^{4}He. This non-radiation anomaly is covered in the "Discussion".

Cluster imploding EM pulse

The nature of the transient imploding electric field pressure pulse shows up as a spherical compression movement that squeezes the contents of the deuteron cluster into its fusion mode. As the pulse moves inward, its energy density increases as 1/Radius cubed. As the cluster density increases, so does the escape pressure. A cluster radius reduction of 10 times corresponds to a volume change of 1/1000. Resisting this compression is the nearly constant coulomb repulsion of the surface deuterons from the cluster The escape pressure is not constant but should be close to 10^{13} bars for the 1 million deuteron cluster with an initial

density of 10^{27} D^{+}/cc. The compression of the imploding pulse is an increasing pressure wave approaching a picosecond in length. This compression pressure is in the range of 10^{23} bars. So escape pressures do not detract from the cluster compression during this short period of around a picosecond. About 50% of the surface atoms are converted to deuterium atoms that produce their evapoated cluster cooling and the EM imploding pressure pulse.

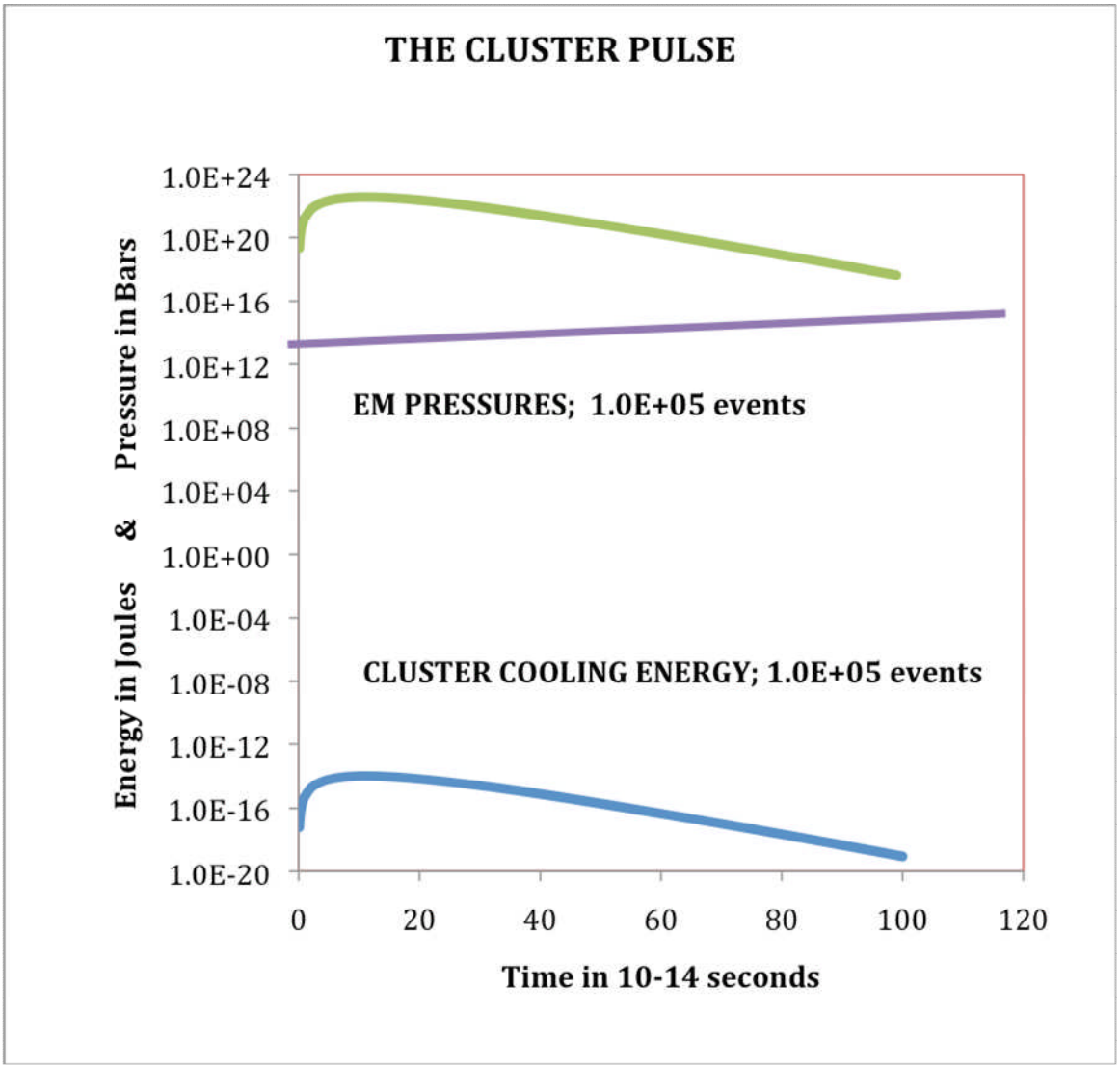

Figure 10. Two important aspects of one-million deuteron cluster's mechanism, cooling and compression by the implanted free electrons. Removing heat and EM pressure pulse was produced as free electrons from their position in the lattice accelerated to the positively charged cluster surface. The EM pressure pulse to the point of DD fusion, the green line, further compressed the already dense deuteron clusters located in the target foil. Note the purple line is the escape pressure of the cluster deuterons via their coulombic repulsion pressure that is much smaller than the EM compressing pressure pulse during that initial picosecond following the jet implant. Compression occurs while maintaining a relatively cool temperature of 4000 K [1]. During the EM spherical implosion pulse the cluster temperature is moderated by the evaporation of cluster's surface deuterons, blue line. The EM compressing pressure is shown in figure 4 and the compression heating may eventually overtake evaporative cooling. The E pulse as it moves to the center of the cluster gains energy density as it squeezes the cluster contents.

During the adiabatic compression the evaporated deuteron has a femtosecond recombination time as a cluster surface deuteron captures a free implanted electron drawing 14.7 eV of heating in a zone away from the BEC cluster. For example, the evaporation of 10^5 from a 10^6 deuteron cluster in a picosecond relates to an energy of 2.3×10^{-13} Joules that are removed from the cluster during its existence. This energy is enough to reduce the BEC superconducting cluster delta temperature of 10^5 K during its transient compression pulse. The evaporation momentum is added to the compression forces. The temperature is well below its BEC Tc phase temperature and in its ground state level. (The cluster's deuteron nuclear energy states are separated by MeV levels.)

Summary

Examining the macro world of sonofusion, bubbles, acoustic input, target foils, D_2O flow, temperature, pressure, and SEM ejecta sites and apply it to a nano world of atoms, molecules, ions, electrons, moving charges, imploding electric fields, BEC, superfluids, coherence, and the femtosecond evaporation of cooling deuterium atoms. Looking into the heart of the cluster system and finding a picosecond star-like object called a boson cluster where single and multiple fusion events occur, producing ^{4}He, Qx, and ejecta sites. These clusters can relate to the number of fusion events found in SEM photo surveys of ejecta site populations.

This paper is speculative looks to explain the experimental results via high density and low temperatures of SF systems developing important paths in the transient SF cluster. Increasing the cluster density, keeping its temperature low, using higher frequency piezos, and decreasing the size of the SF device are good guidelines for future progress in the alternate energy SF search. An attempt has been made to look for a path that incorporates most of the experimental technology called micro fusion, bubble fusion, and SF into a reasonable model of what today is called SF. Transient cavitation bubbles create plasma jets that implant target foils producing fusion events in transient deuteron clusters that terminate in a fusion heat pulse (excess heat, Qx). See figure 10. The technologies of SF, ICF, MF, EMF, frozen deuterium HDZP implosions, imploding wire (with a flow of electrons producing magnetic fields strong enough the turn wires to dust), and the low temperature studies of Bose Einstein Condensate and Bardeen Cooper, Schrieffer systems and their crossover relationships are related technologies that are helpful to the understanding of electromagnetic compressive and evaporative pressures that confine SF jets and clusters. These technologies have been applied to much smaller SF systems of a million or so particles. The varied technologies are useful, when applied to all hydrogen isotope systems. Frozen D_2 and DT fibers, ~50 µm diameter, in the high-density z pinch experiments, are 9 to 17 orders of magnitude higher in volume than found in the SF jet and cluster. Note, compared to 1.6 MHz SF jet volume of 10^{-24} m^3 to the jet at a lower frequency of 20 KHz the jets systems are 1000 larger and the number of deuterons in a cluster is smaller as the frequency increases. The z-pinch is still a developing technology, and receives funding from many governments. The z-pinch problem is now part of the solution for the SF mechanism, particularly the SF jet and cluster. The SF cluster gains support from the laser impacted deuterium tritium in the ICF capsules. The SF cluster also gains support from the boson deuteron BEC and its MeV separation of excited nuclear energy states of hydrogen ion isotopes. And support from the evaporative cooling gives the necessary cluster temperature control. The 32,000 K is far below the MeV values for excited states of the electron free deuteron nucleus. This makes the BEC Qx fusion product feasible rather than gamma radiation. Several inputs from hot fusion research, astrophysics, and low temperature condensates add to the development of SF technology. These other disciplines of physics, such as MF, help explain SF products. SF is a complex series of interlocked events produced by the acoustic driven collapse of a TCB collapse that result in propagation of the jet plasma and cluster.

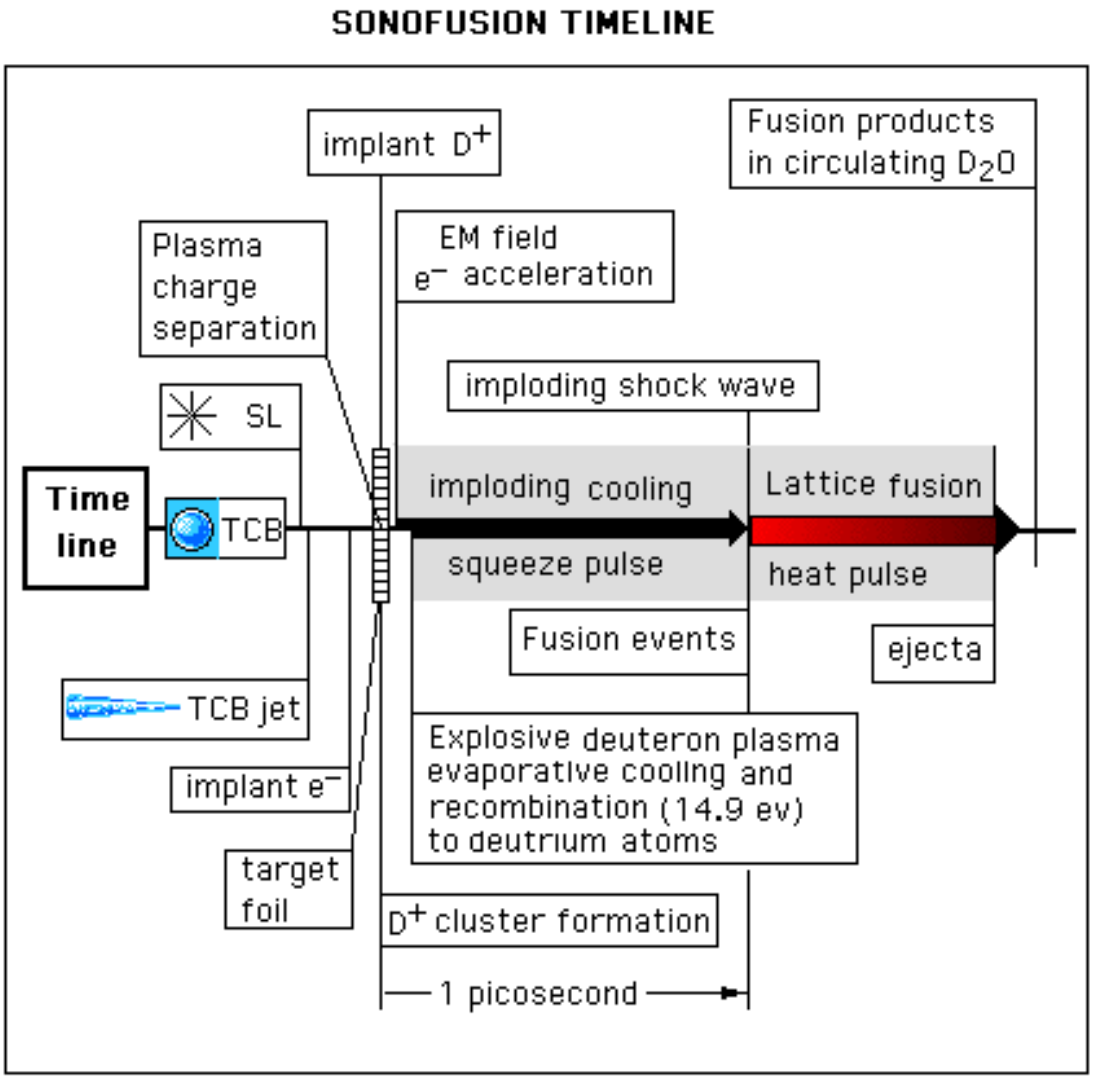

Figure 11. The sequence of events in a timeline of a TCB adiabatic bubble collapse producing sonoluminescence and a high-density deuteron jet. The plasma jet is accelerated and further compressed by its z-pinch. The jet reaching the target foil implants electrons into the target foil followed by the implant of deuterons that are pushed by electrons into clusters. The time line is keyed to the cluster's 1 picosecond lifetime. The cluster's surface deuterons immediately attract the mobile electrons producing the EM implosion pulse and the cooling via deuteron evaporation from the cluster surface. The pulse produces a shock wave front in the BEC cluster where the DD fusion event occurs. The fusion heat pulse is larger than the EM implosion heat pulse. The fusion heat pulse spreads spherically in the target lattice to the target foil surface where it ejects vaporous lattice and fusion products, ^{4}He and Qx, into the circulating D_2O. Left behind in the target foil lattice is an ejecta site that is proportional in size to the number of fusion events that occurred in the deuteron cluster. Ejecta sites are the result of the spherical fusion heat pulse reaching the target foil surface and leave in the target lattice a permanent record of the number fusion events in a cluster. Ejecta sites are observed and measured by SEM photos as frozen entities in target foils.

The jet plasma can be described as a nano-scale transient plasma of 10^7 particles at astrophysical densities. Jet target implantation produced an initial charge separation of free electrons and deuteron cluster(s). An evaporative cooling of deuterium atoms immediately cools the cluster as it compresses. An EM compression shockwave to compress a BEC coherent cluster squeezes two deuterons into a fusion event.

The clusters in the target lattice fuse deuterons with the resulting heat pulse and ejecta and close out or finish the single cycle of a one bubble system while providing seeds for the next acoustic cycle and its millions of new bubbles. A timeline for a single cluster event is presented in figure 11. The fusion products of SF are ^{4}He and Qx and are discharged into the circulating D_2O. Qx amounts to 40 watts for the 1.6 MHz SF system [12].

Mixed hydrogen isotope cavitation systems and the produced SF clusters. Look at some astrophysical systems and their fermions and bosons and their relation to a white dwarf star's gravitational forces that act on changing densities during the WDS collapse mode that must find a new point of equilibrium because of the cut off of its radiation pressure. Those new equilibrium pressures are very close to MF densities and are approached by SF transient densities. The transient compression of a SF cluster consisting of bosons, fermions, or a combination, where two fermions combine, produce a boson found in the BEC-BCS crossover process. The bosons of the SF cluster have a degenerate singular BEC energy state in the MeV range. With tuned magnetic fields these bosons can cross over reverting back to fermions. This may be happening in clusters with atoms and ions of hydrogen isotopes. Processes are occurring in the mass of the white dwarf star that changes its fermion boson numbers to reach an equilibrium balance between gravitational and fermion pressures that one might find in the BCS-BEC crossover systems with the formation of Cooper pairs. This is usually accomplished using a magnetic resonance input but in SF the picosecond lifetime allows for only the initial fermion boson cluster formation or does it. Fermion systems may cross over into boson systems to become boson clusters. The effect of the Pauli Exclusion Principal on the mass of the white dwarf star limits the density of its mass where the fermions limit the gravitational collapse in the WDS. This involves the spin of the particles that may change when they combine from fermions to bosons, endothermic and evaporative cooling, or visa versa in crossover environments present in high-density systems. The cluster composition of hydrogen isotopic ions of different spins can be applied to a SF cluster with the result of fusion products other than ^{4}He. It should be emphasized that SF is a natural process and just needs guidance and understanding to produce fusion.

Acknowledgements

I would like to thank Julie Wallace, Dick America, Jim Rieker, and Brian Marcus.

Appendix - A list of symbols

(A)	20 KHz SF system
(B)	46 KHz SF system
A	area
B	magnetic field
BCS	Bardeen, Cooper, Schriffer
BDS	black dwarf star
BEC	Bose Einstein Condensate
(C)	1600 KHz SF system
D	deuterium atom
D+	deuteron
dB	de Broglie wavelength
DDμ	molecular ion of deuterium atoms
□Tss	Tout-Tin in Kelvin steady state
E	electric field
e-	electron
EM	electromagnetic
ev	electron volt
FMI	pumps based on moving volume D_2O
HDZP	high-density z-pinch device [13]
ICF	inertial confined fusion
k	Boltzmann constant
MF	muon fusion
MS	Mass spectral analysis
N	num. D^+ converted to D atoms
n	number of particles
PB	magnetic field pressure
Pe	deuteron escape pressure
PE	electric field pressure
PMT	photomultiplier
Qa	acoustic watts input
Qi	SF total input watts
Qo	heat out of the SF device in watts
Qx	Excess heat in watts
SEM	Scanning Electron Microscope
SF	sonofusion
SL	sonoluminescence
SRI	Stanford Research International
T	temperature
Tc	temperature of BEC phase change
tf	cluster's final time
ti	cluster's initial time
ve	velocity of electron
WDS	white dwarf star

References

1. R. Stringham, ICCF-14 Proceedings, Ed. by D. Nagle and M. Melich Ed, Washington DC, 10 – 15 Aug. 2008 to be pub. ACS LENR Source Book, Vol. 2, J. Marwan and S. Krivit Ed. to be publ.
2. J. E. Miraglia, Phys. Rev. A, vol 1, 32, 2702-05 (1985)
3. M. A. Liberman, J. S. De Groot, A. Toor, R. B. Spielman; Physics of High-Density Z-Pinch Plasmas; Springer-Verlag NY, QC718.5.P45P48, 1998, page 37.
4. L.W. Alvarez, et al, Catalysis Nuclear Reactions by μ Mesons, 1957, Phys. Rev.;105 1127.
5. S. S. Botelho, Georgia Tech. Univ., thesis and dissertations, BCS to BEC, 12 Sept. 2005.
6. R. D. Petrasso, et al, Proton Radiography of Inertial Fusion Implosions, 29 Feb. 2008, Science, 319: 1223-1225
7. M. P. Brenner, S. Hilgenfeldt, and D. Lohse, 2002, Rev. of Modern Phys., vol 74, No 2; 425-484
8. R. Stringham, ICCF-8 Proceedings, Villa Marigola, LaSpezia, Italy, May 2002, 299- 304. and see web LENR CANR web Author; R. Stringham, March 12 to 17, 2007, DVD presentation "1.6 MHz Sonofusion Measurement and Model, 2007, APS meeting, Denver, CO. R. Stringham, ICCF-10 Proceedings, Poster, P. Haglestein, S. Chubb ed. Boston, USA, LANL-CANR web library. 2003
9. R. Stringham, ICCF-8 Proceedings, F. Scaramuzzi ed. Lerici, LaSpezia, Italy, 21-26 May 2000, 299-304.
10. Y. Tomita, A. Shima; Acoustica, 1990, 71,161. and M. P. Felix, A. T. Ellis, Appl. Phys. Lett. 1971, 19, 484, and W. Lautterborn, H. Bolle, J. Fluid Mech., 1975, 72, 391.
11. R. Hickling, Phys. Rev. Lett., 1994, 73(21), 5853.
12. R. Stringham, ACS Publications "Low-Energy Nuclear Reactions Sourcebook (Volume 2)", Ed Jan Marwan and Steve Krivet, to be published in 2009.
13. M. A. Liberman, J. S. De Groot, A. Toor, R. B. Spielman; Physics of High-Density Z-Pinch Plasmas; Springer-Verlag NY, QC718.5.P45P48, 1998, page 19 and 238-241.
14. Double layer or multi layer refers to a structure of a plasma with parallel plasma layers with opposite charges. Wikipedia. http://en.wikipedia.org/wiki/Double_layer_(plasma)
15. The Alfven waves and jets recently described from measurements made by the Hinode solar telescope, 7, Dec. '07, Science , vol 138, 1571
16. K. R. Weninger, P. G. Evans, and S. J. Putterman, Phys. Rev. E. 2000, 61(2), 3.
17. S. Chubb, T Chubb, P. Hagelstein, Y. Kim and others who have presented theories on why gammas are not present, most recently at the Proceedings of ICCF 12, Nov.-Dec. 2, 2005, A. Takahashi ed. Yokahama, Japan.
18. A. A. Isayev, JETP Lett., 2005, vol 82, No 9, 551556
19. Brian Oliver; DOE MS analysis of ^{4}He & ^{3}He in target metals for EQuest Sciences, report, "HELIUM ANALYSIS OF TARGET METALS" B. M. Oliver, 1995, Rockwell, International, Canoga Park, CA 91309.